RSC Advances

PAPER

View Article Online
View Journal | View Issue

Cite this: *RSC Adv.*, 2023, **13**, 36439

Iodine catalyzed synthesis of imidazo[1,2-*a*]pyrazine and imidazo[1,2-*a*]pyridine derivatives and their anticancer activity†

Rajavenkatesh Krishnamoorthy *[a] and Parthiban Anaikutti *[b]

Received 16th November 2023
Accepted 6th December 2023

DOI: 10.1039/d3ra07842f

rsc.li/rsc-advances

An efficient iodine-catalyzed method for synthesizing imidazo[1,2-*a*]pyrazines and imidazo[1,2-*a*]pyridines *via* one-pot three-component condensations has been reported. The product, generated *in situ* by the reaction between an aryl aldehyde and 2-aminopyridine or 2-aminopyrazine, undergoes [4 + 1] cycloaddition with *tert*-butyl isocyanide, affording the corresponding imidazopyrazine and imidazopyridine derivatives in good yields. The photophysical properties of these new fluorescent derivatives are also presented. The anti-cancer activities of the synthesized compounds (**10a–m**) and (**12a–l**) were evaluated against four cancer cells (Hep-2, HepG2, MCF-7, A375) and the normal Vero cell. Significant anti-cancer activities were observed and compared with the standard drug Doxorubicin. *In vitro* experimental results revealed that compound **12b** is a promising lead with IC_{50} values of 11 μM, 13 μM, 11 μM, 11 μM, and 91 μM against Hep-2, HepG2, MCF-7, A375, and Vero, respectively.

Introduction

With improper and uncontrolled cell division, cancer encompasses over 100 diseases affecting the body extensively. Globally, cancer ranks as the second leading cause of mortality, accounting for 1 in 6 deaths in 2018, totaling 9.6 million deaths.[1] Diverse malignancies impact both genders. Current anti-cancer medications exhibit distinct modes of action, leading to varying effects on cancer types and healthy cells.[2] Moreover, limited evidence distinguishes malignant cells biochemically from normal ones, impeding targeted treatments.[3] A critical concern is cancer's resistance to multi-drug chemotherapy, coupled with poor cure rates, severe side effects, and patient harm. Thus, vital for cancer treatment, the development of superior, more efficient, and less harmful chemotherapeutic drugs remains imperative.[4]

Multicomponent reactions (MCRs) offer simple and atom-economical methods for synthesizing complex molecular structures with a wide range of biological activities.[5] Consequently, product purification resulting from MCRs becomes simpler, as almost all starting materials are incorporated into the formed product. Additional advantages of MCRs, such as being less time-consuming and facilitating diversity-oriented synthesis with good yields, have captured the attention of chemists, particularly for the synthesis of biologically active complex molecular structures. Therefore, the development of environmentally friendly and efficient MCRs is acknowledged as a critical topic in green chemistry.

Nitrogen-containing heterocyclic compounds have attracted significant interest due to their broad range of applications, especially in biomedicine. Within this context, isocyanide-based MCRs like Ugi-3CRs, Ugi-4CRs, and Passerini reactions have been employed to synthesize structurally diverse small molecule libraries.[6] Among the wide spectrum of nitrogen heterocyclic compounds, imidazo[1,2-*a*]pyrazine and pyridines hold importance as a class of bridgehead heterocycles. Notable drug candidates within this class include zolpidem (**1**), alpidem (**2**), saripidem (**3**), olprinone (**4**), zolimidine (**5**), and ND-009628 (**6**) (Fig. 1). These compounds exhibit various pharmacological properties, such as sedative-hypnotics as well as antibacterial,[7] antifungal,[8] antiviral[9–12] and anti-inflammatory[13,14] activities. The inhibitory effects of imidazo[1,2-*a*]pyrazines against insulin-like growth factor-I receptor (IGF-IR),[15] p13K,[16] aurora kinase,[17] and tyrosine kinase EphB4[18] have garnered substantial attention. Recently, Li *et al.* research groups reported imidazo[1,2-*a*]pyrazines and its analogs shows inhibition of SARS-CoV and SARS-CoV-2 main protease with excellent activity with IC_{50} values as low as 21 nM.[19] Consequently, numerous attempts have been made to synthesize these compounds.[20,21]

Previously reported methods for synthesizing imidazo derivatives using Lewis acid catalysts like $ZnCl_2$,[22] $Sc(OTf)_3$,[23] $MgCl_2$,[24] and $ZrCl_4$[25] suffer from long reaction times and low yields. As a result, the development of new methodologies

[a]*Organic and Bioorganic Chemistry Laboratory, CSIR-Central Leather Research Institute (CSIR-CLRI), Adyar, Chennai, Tamil Nadu-600020, India. E-mail: krajavenkateshcmp5@gmail.com; rajavenkateshk2@gmail.com*

[b]*Centre for GMP, National Institute of Pharmaceutical Education and Research (NIPER-G), Guwahati, Assam-781101, India. E-mail: parthichem84@gmail.com; parthiban@niperguwahati.in; Tel: +91 9843080794*

† Electronic supplementary information (ESI) available: The ^1H NMR, ^{13}C NMR data of all compounds are given. See DOI: https://doi.org/10.1039/d3ra07842f

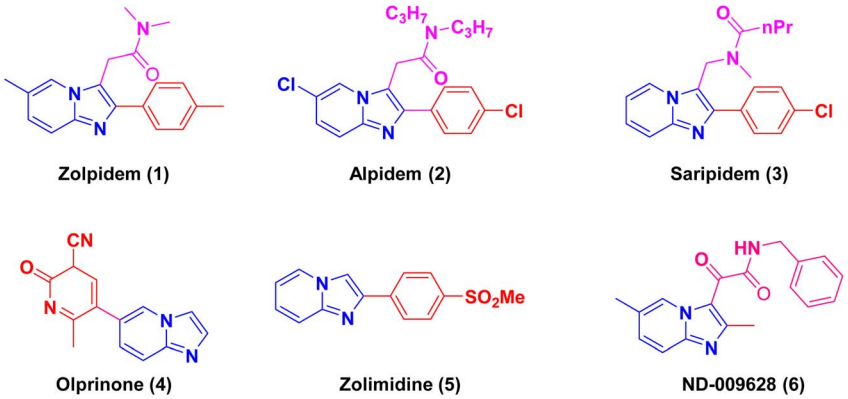

Fig. 1 Examples of anticancer/antiviral/antibacterial activities of imidazo[1,2-*a*]pyridine molecules.

offering cost-effective and eco-friendly procedures with high yields becomes both challenging and imperative. Within this context, we focused on a new methodology that utilizes *tert*-butyl isocyanide-based Ugi-type multicomponent reactions for the efficient preparation of a series of heterocyclic fluorophores with good yields. Iodine serves as a catalyst in the synthesis of imidazo[1,2-*a*]pyrazines and imidazo[1,2-*a*]pyridines, making it a viable choice in MCRs due to its low cost, easy availability, and benign nature.[26] The three-component condensation involving *tert*-butyl isocyanide, an aryl aldehyde, and 2-aminopyridine or 2-aminopyrazine at room temperature leads to the formation of imidazo[1,2-*a*]pyrazine and imidazo[1,2-*a*]pyridine derivatives. Herein, we present this straightforward one-pot synthesis of imidazo[1,2-*a*]pyrazine and pyridine derivatives. The advantage of *tert*-butyl isocyanide-based multicomponent reactions at room temperature is emphasized. To the best of our knowledge, this is the first report where *tert*-butyl isocyanide, an aryl aldehyde, and 2-aminopyrazine or 2-aminopyridine, in the presence of iodine as a catalyst in ethanol, result in highly functionalized imidazo[1,2-*a*]pyrazine and pyridine derivatives with excellent yields. Henceforth in continuation of our efforts in medicinal chemistry research[27] and considering the biological importance of the imidazo[1,2-*a*]pyrazine and imidazo[1,2-*a*]pyridine derivatives,[28] the present work aimed to design, synthesis and biological activity of imidazo[1,2-*a*]pyrazine and imidazo[1,2-*a*]pyridine derivatives by *in vitro* anticancer studies.

Results and discussion

Chemistry

The low yield of the desired compounds in isocyanide-based multicomponent reactions is due to the decomposition of acid-sensitive 2-morpholinoethyl, *p*-methoxyphenyl, trimethylsilyl cyanides and *tert*-butyl isocyanide (at higher temperature).[29] Thus, a pilot reaction involving 2-aminopyrazine **7**, 4-nitrobenzaldehyde **8**, and *tert*-butyl isocyanide **9** was conducted at room temperature for approximately 1 hour in both polar and non-polar solvents, employing 5 mol% of various Lewis acids such as ceric ammonium nitrate (CAN), $SnCl_4$, $SnCl_2$, $InCl_3$, $FeCl_3$, PTSA·H_2O, and I_2 as catalysts to evaluate their efficiency in terms of reaction yield and time (Scheme 1, Table 1). Initially, the reaction was carried out with different catalysts (entries 1–5; Table 1), resulting in moderate yields and however, product has to be isolate in conventional workup and column chromatography. The reaction with ferric chloride ($FeCl_3$) (entry 6; Table 1) yielded poor results. On the other hand, the presence of 5 mol% of I_2 (entry 7; Table 1) as

Table 1 Optimization of reaction conditions[a]

Entry	Catalyst (5 mol%)	Solvent	Time (h)	Yield[b] (%)
1	CAN	EtOH	20	54
2	$SnCl_4$	EtOH	24	58
3	$SnCl_2$	EtOH	24	48
4	$InCl_3$	EtOH	24	55
5	PTSA·H_2O	EtOH	24	75
6	$FeCl_3$	EtOH	24	25
7	I_2	EtOH	5	98
8	I_2	MeOH	15	85
9	I_2	Water	24	80
10	I_2	ACN	30	57
11	I_2	DCM	30	51
12	I_2	Toluene	30	25
13	No catalyst	EtOH	24	—

[a] The reaction was performed using 1.0 mmol each of 4-nitrobenzaldehyde, 2-aminopyrazine and *tert*-butyl isocyanide at room temperature. [b] Isolated yield.

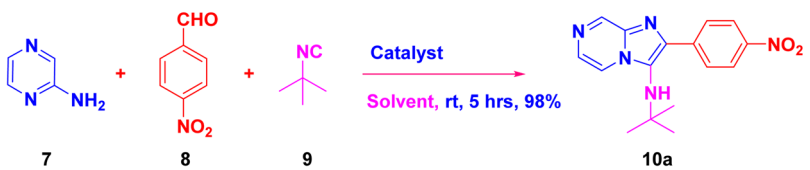

Scheme 1 Schematic diagram of formation of imidazo[1,2-*a*]pyrazines.

a catalyst in ethanol solvent provided excellent yields of imidazo[1,2-*a*]pyrazines with high purity. The reaction was also tested in various solvents such as MeOH, H_2O, ACN, DCM (entries 8–11: Table 1), and the non-polar solvent toluene (entry 12), yielding moderate to low yields. Among the catalysts tested, iodine proved to be cost-effective and eco-friendly for the synthesis of desired product **10a** (Table 1). Further experimentation with 10 mol% iodine did not significantly improve the overall yield. The reaction did not proceed in the absence of iodine in ethanol (entry 13). Based on optimization results, the iodine–ethanol condition was found to be ideal for this three-component reaction, providing an excellent yield. Notably, under the iodine–ethanol condition, the product precipitated in the reaction vessel, simplifying purification through straightforward filtration. Hence, no additional purification techniques were required to obtain the pure desired product **10a**.

The desired product **10a** was characterized by IR, ^{1}H NMR, ^{13}C NMR and ESI-HRMS analysis. FT-IR spectra analysis given that the N–H stretching of amine functional group was appeared strong peak at 3350 cm^{-1} and the UV spectra analysis gave broad absorbance spectrum at 368 nm to confirm that the amine group present in the molecule. The ^{1}H NMR spectra of **10a** revealed that NH proton was appeared at 3.08 ppm as singlet and the *t*-butyl group was observed at 1.09 as singlet. The aromatic pyrazine hydrogen was located at δ 9.03 as a singlet and the remaining two hydrogens were appeared at δ 8.32–8.30 ppm as doublets in pyrazine ring. The four aromatic hydrogens were located in multiplets at 8.30–7.91 ppm (ESI Fig. 1†). The ^{13}C NMR spectrum of **10a** displayed 12 distinct signals, including two aliphatic regions one at 30 ppm that proved *t*-butyl CH_3 carbon and another carbon at 57 ppm that confirmed *t*-butyl quaternary carbon. Total of ten carbons with five CH and five quaternary carbons were appeared in aromatic regions at δ 147.21 to 116.30 ppm (ESI Fig. 2†). The purified imidazo[1,2-*a*]pyrazines **10a** subjected to ESI-HRMS to identify the mass of product and mass calculated for $C_{16}H_{17}N_5O_2$: ESI-HRMS = 312.1460 which was found to be 312.1465 $(M + H)^+$. After optimizing the reaction conditions, we synthesized different imidazo[1,2-*a*]pyrazine derivatives (**10a–m**) using *tert*-butyl isocyanide **9** and appropriate aryl aldehydes **8**. In almost

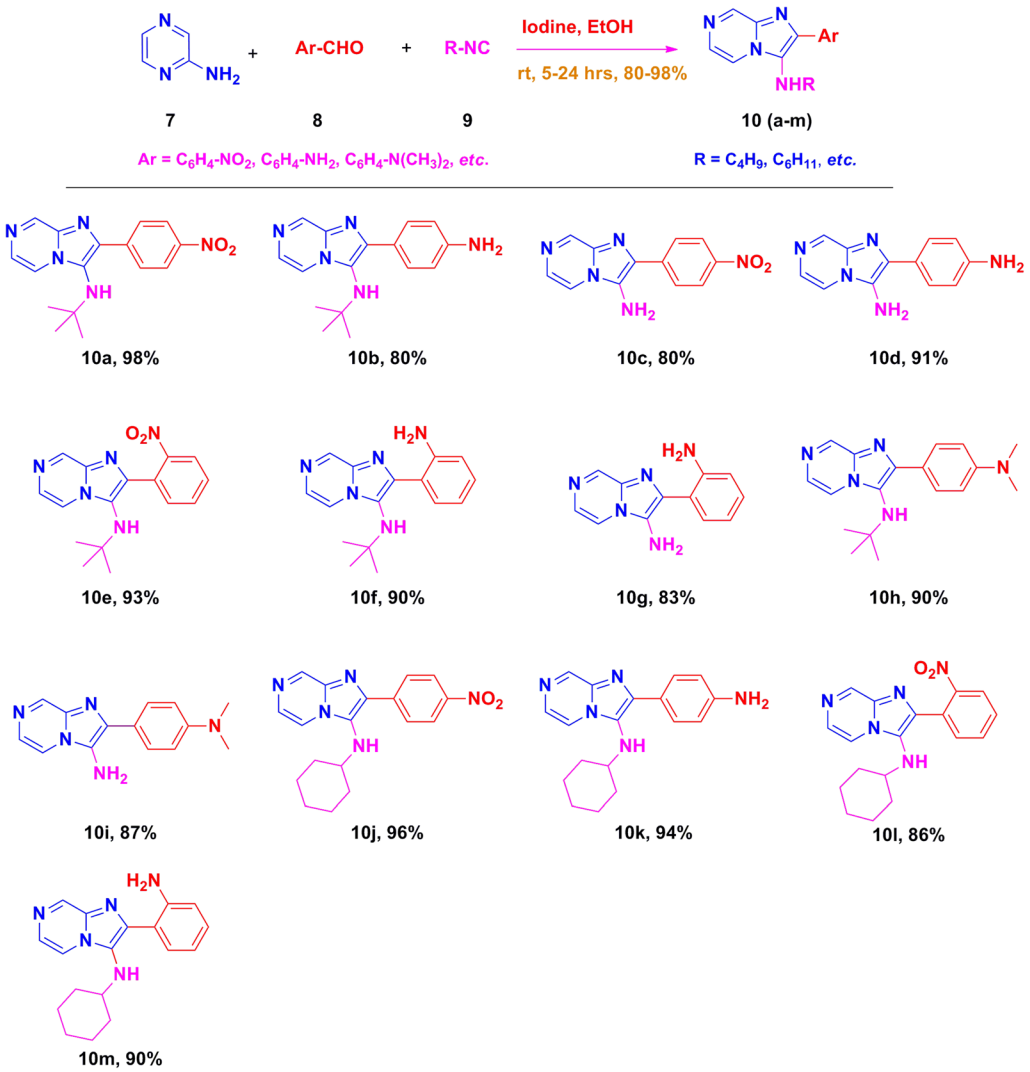

Scheme 2 Library synthesis of imidazo[1,2-*a*]pyrazines derivatives (**10a–m**).

all the cases, the reaction proceeded well and the formations of the cyclized products were in moderate to good yields (ESI Fig. 1–24†). To further expand the scope of this methodology and the catalytic role of iodine, cyclohexyl isocyanide is also used for the synthesis of the corresponding imidazo[1,2-*a*]pyrazine derivatives (**10a–m**) (Scheme 2) in good yields.

To broaden the scope of this room temperature protocol, the one-pot reaction involving 2-aminopyridine **11**, *tert*-butyl isocyanide **9** and different aryl aldehyde **8** was carried out. Iodine effectively catalyzed the cyclo-condensation of different aldehydes with 2-aminopyridine and *tert*-butyl isocyanide resulting in the corresponding 3-aminoimidazo[1,2-*a*]pyridines (**12a–l**) (Scheme 3) in good yields (ESI Fig. 25–50†). The HPLC spectrum analysis of the most potent compounds (**10b** and **12b**) were carried out on reverse phase C18 column using $CH_3CN : H_2O$ (50 : 50, 1 : 1) as a mobile phase and we obtained more than 98% purity of the samples (ESI Fig. 51 and 52†).

After optimizing the reaction conditions, a plausible mechanism is presented in Scheme 4. In the initial step, condensation of 2-aminopyrazine **7** or 2-amino pyridine **11** with an aryl aldehyde **8** yields the formation of the imine ion A. This ion is subsequently activated by the Lewis acid iodine, facilitating the nucleophilic addition of *tert*-butyl isocyanide **9**. This addition leads to the creation of the intermediate iminium ion B. The nucleophilic addition of *tert*-butyl isocyanide **9** to intermediate B undergoes [4 + 1] cycloaddition generates intermediate C. Finally, intramolecular interaction involving the nitrogen of the pyrazine or pyridine ring in intermediate C propels the entire reaction towards the formation of cyclized products imidazopyrazine **10** and imidazopyridine **12**, as anticipated in Scheme 4.

By using this methodology, we have synthesized nitro substituted imidazo[1,2-*a*]pyrazines (**10a**, **10c**, **10e**, **10j** and **10l**) and imidazo[1,2-*a*]pyridine derivatives (**12a**, **12c**, **12e**, **12g** and **12k**). According to the literature, the nitro group containing molecules act as both a pharmacophore as well as toxicophore and making it even much more fascinating for medicinal chemists.[30] In most cases, the nitro group containing compounds were showed lesser anticancer activity and also affect fluorescent properties. In order to increase anticancer as well as fluorescent properties,[31] we have carried out reduction process with those compounds using $H_2N–NH_2$, Pd/C afforded amine containing imidazo[1,2-*a*]pyrazines (**10b**, **10d**, **10f**, **10k** and **10m**) and imidazo[1,2-*a*]pyridine derivatives (**12b**, **12d**, **12f**, **12h** and **12l**) with good yields. Using TFA : H_2O (9 : 1) and followed by adjust pH using NaOH with EtOH (to avoid TFA-amine formation) compounds **10a**, **10b**, **12a** and **12b** having the NH-attachment of *t*-butyl group was deprotected and gives **10c**, **10d**, **12c** and **12d** compounds.[32] The general procedure for synthesizing derivatives (**10b–d**) and (**12b–d**) is presented in Scheme 5.

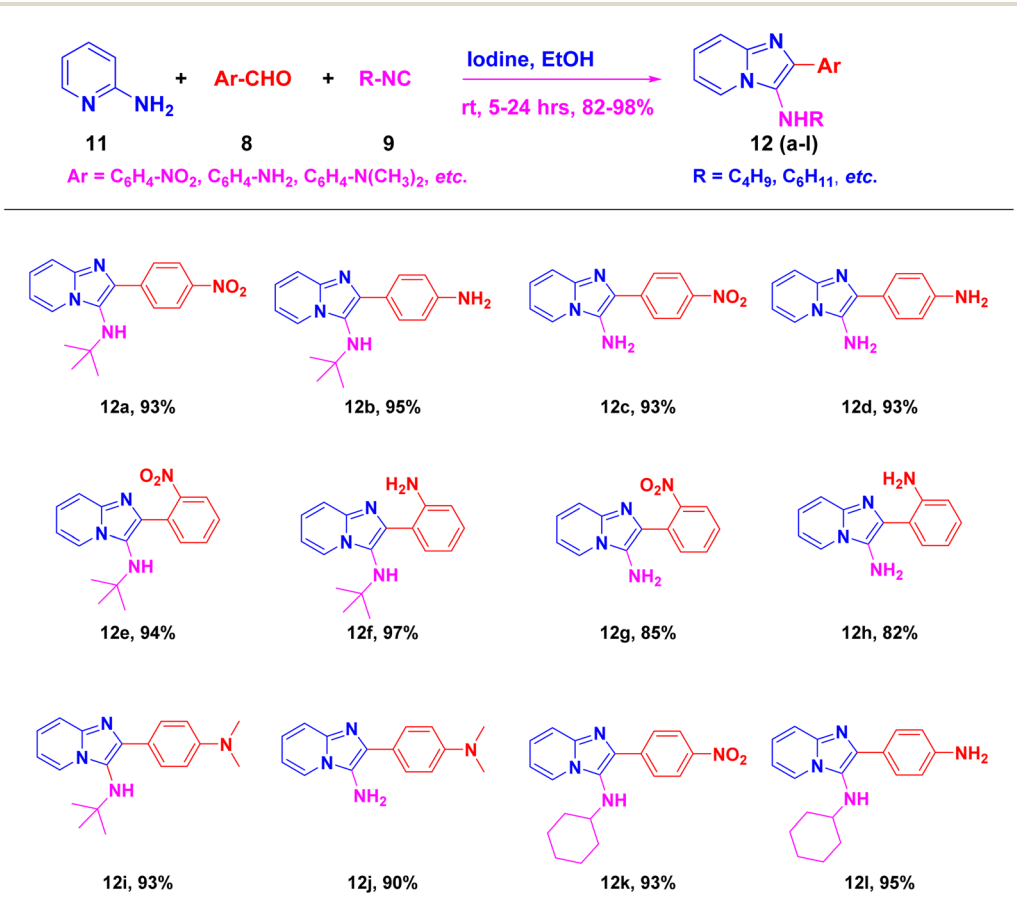

Scheme 3 Library synthesis of imidazo[1,2-*a*]pyridines derivatives (**12a–l**).

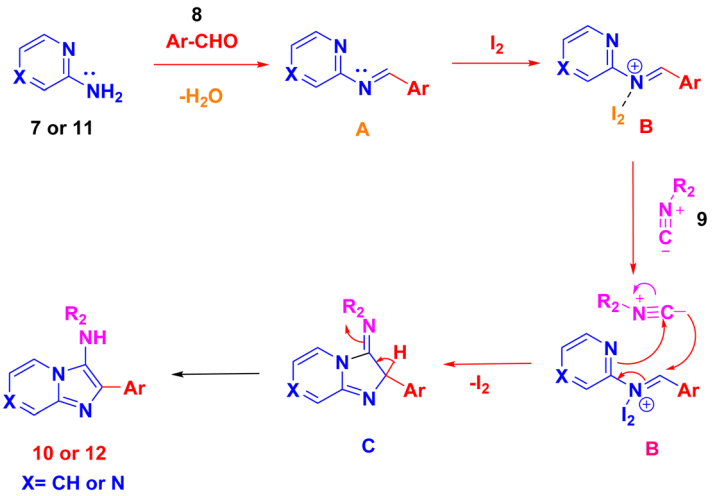

Scheme 4 Plausible mechanism for formation of compounds (10 and 12).

Considering the significance of fluorescent molecules acting as chemosensors and biosensors.[33–35] The absorption and fluorescence characteristics of all compounds were investigated in media of different polarity. Among the derivatives, **10b**, **10i**, **12b** and **12i** exhibited more favorable fluorescence emission spectra compared to the other compounds. Consequently, these specific compounds were chosen for further biological evaluation based on their recorded fluorescence spectra. Among the solvents tested, acetonitrile displayed the maximum blue shift in emission (Fig. 2). Therefore, acetonitrile was selected as the solvent for measuring the fluorescence characteristics of imidazo[1,2-*a*]pyrazine and pyridine derivatives **10b**, **10i**, **12b**, and **12i**. The absorbance and fluorescence characteristics are significantly influenced by the nature of functional groups (Fig. 2) present at the 2-position in the aryl ring of the imidazo [1,2-*a*]pyrazine and pyridine system. From this data, it can be observed that compound **10i** (which has an additional nitrogen atom in the pyrazine ring compared to **12i**'s pyridine ring) exhibited the maximum emission at ~850 nm, surpassing other derivatives such as **10b**, **12b**, and **12i**.

Anticancer activity

The *in vitro* anticancer properties of all synthesized imidazo[1,2-*a*]pyrazine (**10a–m**) imidazo[1,2-*a*]pyridine (**12a–l**) compounds were screened against four cancer cell lines such as laryngeal carcinoma cell line (Hep-2), hepatocellular carcinoma cell line (HepG2), human skin cancer cell line (A375) and breast cancer cell line (MCF-7) cell lines and the cytotoxicity to the non-cancerous normal cell (Vero) by MTT assay.[36] The compounds were examined for *in vitro* cytotoxicity utilizing a panel of cancer cell lines and a 3-[4,5-dimethylthiazol-2-yl]-2,5-diphenyl tetrazolium bromide (MTT) reduction test for 48 hours. These findings prove the synthesized compounds have anti-proliferative properties. Among other compounds, 2-(4-aminophenyl)-*N*-(*tert*-butyl)imidazo[1,2-*a*]pyridin-3-amine (**12b**) was found to be most potent compound, with IC_{50} values of 11 μM (Hep-2), 13 μM (HepG2), 11 μM (MCF-7), 11 μM (A375) and 91 μM (Vero) cells lines, respectively. These values are almost comparable to the inhibitory value of the standard drug, Doxorubicin IC_{50} values of 10 μM (Hep-2), 1.5 μM (HepG2), 0.85

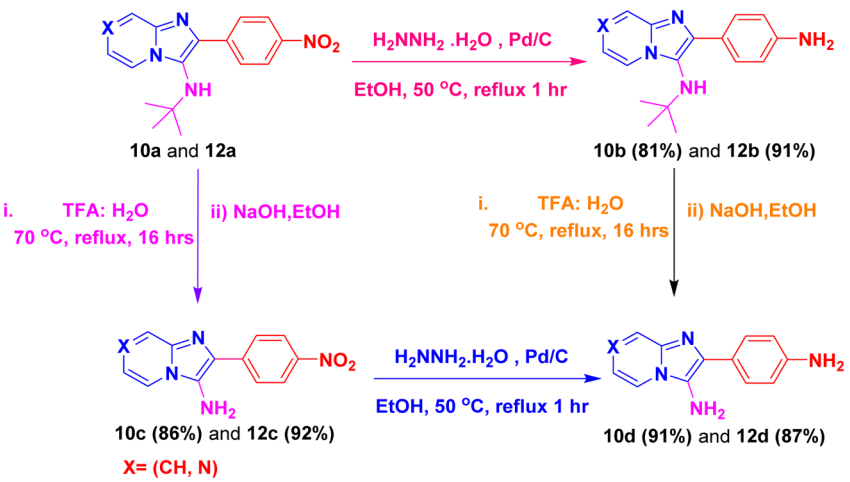

Scheme 5 General schematic line synthesis of compounds (10b–d) and (12b–d).

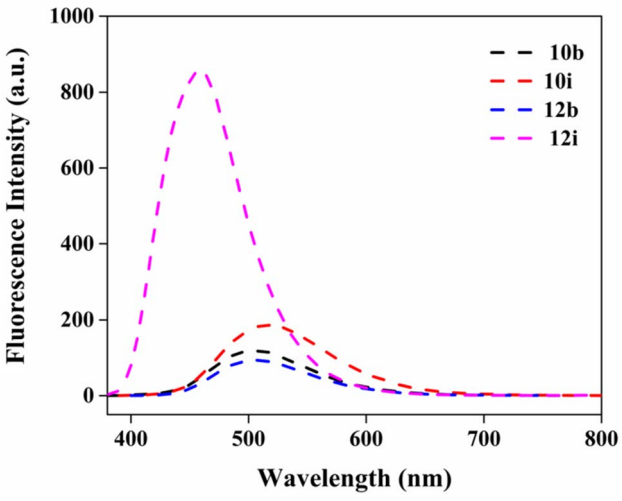

Fig. 2 Fluorescence spectra of imidazo[1,2-*a*]pyrazine and pyridine derivatives **10b**, **10i**, **12b** and **12i** (1 μM) in acetonitrile.

μM (MCF-7), 5.16 μM (A375) and 14 μM (Vero) cells lines (Table 2). From the interpretation of results, the structure–activity relationship (SAR) has been drawn and graphically represented in Fig. 4. It is evident that the central core, imidazo[1,2-*a*]pyrazine and pyridine is an essential requirement for displaying the anticancer activity. The first imidazo[1,2-*a*]pyrazine series (**10a–m**) involves the intact imidazopyrazine skeleton scaffold with variations of electron-donating functional amine groups *viz.* are NH_2, cyclohexylamine, and *tert*-butylamine on the 3rd position of imidazo[1,2-*a*]pyrazine molecules. Among these molecules, the compound **10b** has shown good IC_{50} at a μM concentration against all the cell lines 20 μM (Hep-2), 18 μM (HepG2), 21 μM (MCF-7), 16 μM (A375), 76 μM (Vero) respectively due to increasing order electron-donating nature of *tert*-butylamine when compared than cyclohexylamine **10k** and parent amine **10d** containing imidazo[1,2-*a*]pyrazine compounds. Similarly, **10i** has retained decent activity against two cell lines with IC_{50} values of 17 μM (MCF-7) and 16 μM (A375), respectively, because of electron-donating groups such as *tert*-butylamine at 3rd and *N*,*N*-dimethyl aniline attached at 2nd positions of imidazo[1,2-*a*]pyrazine. Due to electron-donating nature of *tert*-butylamine at the 3rd position and amine located at the steric *ortho* position, the resulting molecule **10f** was showed moderate activity with values of 25 μM (Hep-2), 20 μM (HepG2), 26 μM (MCF-7), 20 μM (A375) and 85 μM (Vero) respectively. Similar to the functional group

Table 2 Anticancer activity of imidazo[1,2-*a*]pyrazine (**10a–m**) and imidazo[1,2-*a*]pyridine (**12a–l**) derivatives[b] from their IC_{50} (μM) values[a]

		In vitro studies				
		Anticancer (IC_{50})[b] (μM)				
S. no.	Compounds	Hep-2	HepG2	MCF-7	A375	Vero
1	**10a**	50 ± 3.42	40 ± 2.52	>100	36 ± 3.1	80 ± 5.72
2	**10b**	20 ± 1.64	18 ± 1.32	21 ± 1.64	16 ± 0.96	76 ± 40
3	**10c**	45 ± 1.6	30 ± 1.43	40 ± 3.8	24 ± 2.48	80 ± 6.72
4	**10d**	38 ± 2.2	34 ± 2.64	30 ± 3.32	25 ± 1.45	96 ± 14
5	**10e**	80 ± 1.37	40 ± 2.52	100 ± 8.64	34 ± 3.2	>100
6	**10f**	25 ± 5.2	20 ± 4.64	26 ± 2.38	20 ± 1.57	85 ± 0.22
7	**10g**	22 ± 2.15	25 ± 4.54	30 ± 1.24	20 ± 5.8	78 ± 5.0
8	**10h**	45 ± 0.5	34 ± 5.5	50 ± 6.41	30 ± 2.84	>100
9	**10i**	28 ± 3.1	26 ± 0.9	17 ± 0.52	16 ± 1.20	91 ± 38
10	**10j**	44 ± 6.4	40 ± 1.4	24 ± 0.15	25 ± 5.41	64 ± 64
11	**10k**	34 ± 4.56	28 ± 2.48	65 ± 2.41	30 ± 1.5	75 ± 2.8
12	**10l**	64 ± 2.45	32 ± 4.64	80 ± 4.53	27 ± 5.0	67 ± 4.54
13	**10m**	28 ± 4.28	20 ± 2.15	44 ± 2.68	23 ± 1.5	75 ± 2.8
14	**12a**	32 ± 5.5	30 ± 2.5	55 ± 5.25	45 ± 2.5	85 ± 14
15	**12b**	11 ± 0.8	13 ± 1.2	11 ± 0.5	11 ± 0.07	91 ± 45
16	**12c**	35 ± 2.4	48 ± 4.8	>100	50 ± 1.8	74 ± 58
17	**12d**	20 ± 5.8	35 ± 2.5	50 ± 1.82	38 ± 2.4	88 ± 85
18	**12e**	55 ± 0.4	62 ± 4.8	>100	>100	78 ± 28
19	**12f**	28 ± 5.0	32 ± 0.1	24 ± 5.8	28 ± 1.5	90 ± 58
20	**12g**	50 ± 5.2	>100	>100	62 ± 2.4	65 ± 14
21	**12h**	44 ± 1.4	54 ± 1.5	61 ± 2.4	55 ± 1.5	74 ± 50
22	**12i**	20 ± 2.7	19 ± 1.3	17 ± 0.92	12 ± 0.7	87 ± 50
23	**12j**	45 ± 5.0	35 ± 4.8	30 ± 5.0	25 ± 1.4	70 ± 12
24	**12k**	30 ± 8.0	40 ± 1.5	52 ± 0.8	41 ± 5.0	85 ± 02
25	**12l**	20 ± 5.2	25 ± 0.2	35 ± 1.5	30 ± 0.1	90 ± 10
26	Doxorubicin	10 ± 0.5	1.5 ± 0.09	0.85 ± 0.02	5.1 ± 0.12	14 ± 10

[a] The cytotoxic effect of compounds against human tumor cell lines was determined by a rapid colorimetric assay, using MTT (5 mg ml^{-1}) and compared with untreated controls. [b] Results are the average of three independent experiments. Hep2-laryngeal carcinoma; HepG2-hepatocellular carcinoma; MCF-7-breast carcinoma; A375-human skin cancer; non-cancerous normal Vero cell. Full detailed experimental procedure has been given in experimental section.

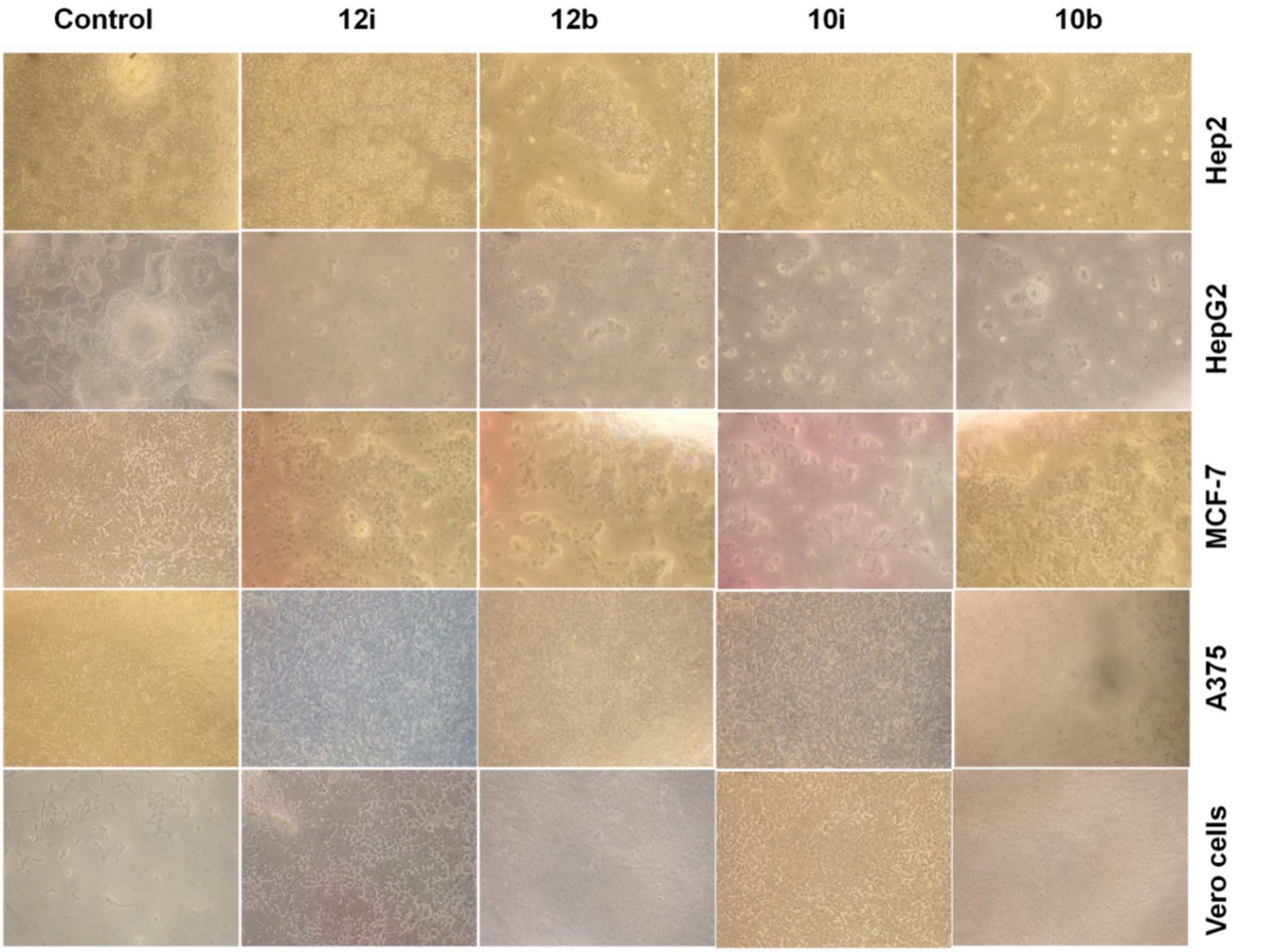

Fig. 3 Cell viability assay (up to 100 μM): normal Vero cell and cancer cells (Hep-2, HepG2, A375, and MCF-7) showing no cytotoxic effects against normal cells. Scale bar = 20 micrometer.

differences, the compounds obtained from the structural dissimilarities on the 2nd position of imidazo[1,2-*a*]pyrazine molecules could not help to increase the activity. For example, the electron-withdrawing group nitro-substituted compounds **10e** and **10l** at meta positions of phenyl rings showed lesser anti-cancer activities and lost two folds its activity than nitro group substituted at para position compounds such as **10a**, **10c** and **10j** owing to steric hindrance between the nitro group and imidazopyrazine ring. The compounds **10g** and **10m** showed significant inhibition against all the cells due to amine substitution at *ortho* position of aryl ring in imidazopyrazine ring. The second category imidazo[1,2-*a*]pyridine compounds (**12a–l**) involves both variations at the substitutions on the 3rd position and 2nd position of imidazo[1,2-*a*]pyridine and showed better anticancer activities similar like imidazo[1,2-*a*]pyrazine series (**10a–m**) owing to electron donating (amines) as well as electron withdrawing groups (NO_2). It is interesting to notice that imidazo[1,2-*a*]pyridine compounds (**12a–l**) is found to have more significant anticancer activities than imidazo[1,2-*a*]pyrazine series (**10a–m**) with the removal of one nitrogen atom at 7th position of imidazole ring. Among both series (**10a–m**) and (**12a–l**), compound **12b**, tertiary butylamine group at 2nd position and phenylamine group at 3rd position showed more substantial anticancer effects with IC_{50} values at 11 μM, 13 μM, 11 μM, 11 μM and 91 μM concentrations against Hep-2, HepG2, MCF-7, A375, and Vero cell lines respectively. Similarly, **12f**, **12i**, and **12l** have displayed better inhibition against the Hep-2, HepG2, MCF-7, A375, and Vero respectively, because of electron donating groups present at 3rd and 2nd position of imidazopyridine ring. The electron withdrawing group bearing compounds **12c**, **12e**, and **12g** exhibited lower inhibition IC_{50} values than electron donating containing compounds **12i**, **12j**, and **12l**. The compound **12b** more preferentially binds to cancer cells' outer membranes *via* electrostatic interfaces and kills the cancer cells from their IC_{50} value Table 2. Therefore, the cytotoxicity of cell viability demonstrates that all compounds (**10b**, **10i**, **12b**, and **12i**) could be utilized to target kill cancer cells while being non-toxic to non-cancerous cells (Fig. 3).

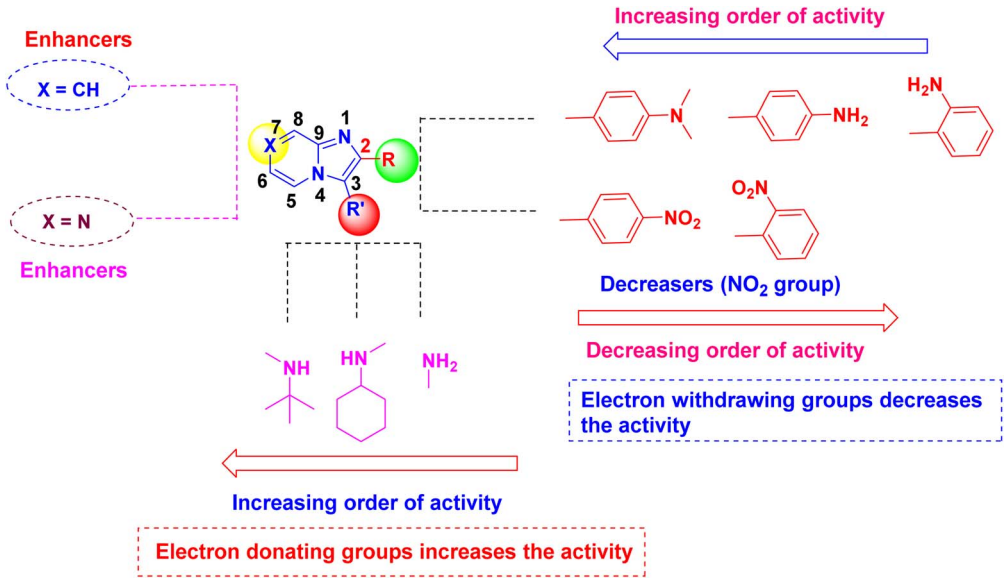

Fig. 4 The anticancer SAR studies of imidazo[1,2-*a*]pyrazine (**10a–m**) and imidazo[1,2-*a*]pyridine (**12a–l**) derivatives.

Conclusions

In conclusion, we have successfully developed an iodine-catalyzed *tert*-butyl isocyanide based three-component condensation at room temperature for the first time. Use of iodine as a catalyst offers a cost-effective method for the synthesis of imidazo[1,2-*a*]pyrazine (**10a–m**) and imidazo[1,2-*a*]pyridine (**12a–l**) derivatives. Compared to *tert*-butyl isocyanide based three-component condensations at higher temperatures, the present methodology offers good yields at room temperature. Simple workup and short reaction time are the other desirable features of this methodology. The compounds **10b**, **10i**, **12b** and **12i** showed better fluorescence emission properties compared to other derivatives. The fluorescent compounds **10b**, **10i**, **12b** and **12i** also show significant anticancer activity against cancer cells. Interestingly, compound **12b** was displayed promising more anticancer activities against the four cancer cells and normal cell, namely, Hep-2, HepG2, MCF-7, A375, and Vero and equated with positive control, Doxorubicin. The compound stability during *in vivo* animal experiments would be major concern when these molecules are considered to deliver small drug molecules. These are the limitations of the present study, and the same aspects are explored currently.

Experimental section

General information

Ethanol (AR grade) and double distilled water were used in all experiments. All the materials for synthesis were purchased from commercial suppliers and used without further purification. Absorption spectra were recorded on SPECORD 200 PLUS and Cary 50 Bio UV-visible spectrophotometer. Fluorescence measurements were performed on a HITACHI F-4500 fluorescence spectrophotometer (Excitation wavelength 355 nm; Slit width 5 nm). NMR spectra were recorded using a Bruker Advance 400 MHz spectrometer operated at 400 MHz. ESI-HRMS spectrum was obtained on a Thermo exactive PE Sciex API3000 mass spectrometer. Further dilutions all measurements were carried out at room temperature. We have prepared 1 μM solutions for the experiments. Stock solutions (1 M) were prepared in de-ionized water. Melting points were determined in open glass capillary with a Stuart scientific SMP3 apparatus and are uncorrected. All the compounds were checked by FT-IR, ^{1}H and ^{13}C NMR and mass spectrometry (Thermo Finningan LCQ-deca XP-plus) equipped with an ESI source and an ion trap detector. Chemical shifts are reported in part per million (ppm). Thin layer chromatography (TLC) was carried out on 5Y 20 cm plates with a layer thickness of 0.25 mm (Merck Silica gel 60 F254).

Materials and methods

Chemical reagents. All reagents were purchased from commercial suppliers and used without further purification. Analytical TLC was performed using silica gel 60 F254 plates. ^{1}H and ^{13}C NMR spectra were recorded using JEOL-ECP500 MHz and Bruker Advance DMX DPX400 MHz spectrometers. The high-resolution mass spectra (HRMS) were recorded on ESI (TOF) MS and CEC-21-110B double focusing mass spectrometer. Absorption spectra were recorded on Specord 200 Plus-223E1271 UV-vis spectrophotometer. Fluorescence measurements were performed on a PerkinElmer LC 45 luminescence spectrometer. HPLC analyses were carried out using the SCL-10ATVP SHIMADZU instrument. HPLC-grade solvents like acetonitrile and water were purchased from Spectrochem. Pvt. Ltd (Mumbai, India). The flow rate was fixed as 0.5 ml min^{-1}, and the UV-detector wavelength was set at 570 nm. The most anticancer active compounds (**10b** and **12b**) were carried out on

reverse phase C18 column using $CH_3CN : H_2O$ (50 : 50, 1 : 1) as an elutant to check the purity of the samples.

MTT-based cytotoxicity assay. The cytotoxic effect of compounds against human tumor cell lines was determined by a rapid colorimetric assay, using 3-(4,5-dimethythiazol-2-yl)-2,5-diphenyl tetrazolium bromide (MTT) and compared with untreated controls. For screening experiment, the cells were seeded in 96-well plates in 100 μL of medium containing 5% FBS, at plating density 10 000 cells per well and incubated at 37 °C, 5% CO_2, 95% air and relative humidity (100%) for 48 h prior to addition of compounds. After 48 hours, compounds at various concentrations were added and incubated at 37 °C, 5% CO_2, 95% air and relative humidity (100%) for 48 hours. Triplicate was maintained and the medium containing without the sample were served as control. After 48 hours, 50 μL of MTT (5 mg ml^{-1}) in triple distilled water was added to each well and incubated at 37 °C for 4 hours. The medium with MTT was then flicked off and the formed formazan crystals were solubilised in 100 μL of DMSO and then measured the absorbance at 570 nm using micro plate reader. The percentage cell inhibition was determined using the following formula and summarized in Table 2.

$$\text{Cell inhibition (\%)} = 100 - \text{absorbance (sample)/absorbance (control)} \times 100$$

Fluorescence studies. Fluorescence measurements were performed on a HITACHI F-4500 fluorescence spectrophotometer (excitation wavelength 355 Slit width 5 nm). UV-vis and fluorescence titrations were conducted using all stock solutions in high concentration to avoid dilution error. Each time, a freshly prepared 3 ml stock solution of imidazo[1,2-*a*] pyrazine and pyridine (1 μM) was taken in the quartz cuvette (path length 1 cm). All measurements were taken at room temperature at 355 nm excitation wavelength by keeping 5 nm as excitation and 5 nm as emission slit width respectively.

General procedure for the synthesis of *N*-(*tert*-butyl)-2-(4-nitrophenyl)imidazo[1,2-*a*]pyrazine and pyridine-3-amine. 4-Nitro benzaldehyde **8** (1.5 g, 10 mmol), 2-amino pyrazine **7** (1.0 g, 10 mmol), or 2-amino pyridine **11** (0.94 g, 10 mmol), tertiary butyl isocyanide **9** (1.2 g, 10 mmol) and ethanol (20 ml) were added to 100 ml RB flask. Iodine catalyst (0.5 mol%) was added and the reaction mixture was stirred at room temperature. The progress of the reaction was monitored through TLC. An orange-yellowish precipitate was formed. After completion of the reaction, the precipitate was filtered off, washed with excess ethanol and dried under vacuum condition. Finally collected the precipitated and crystallized from ethanol to get 3.6 g (98% yield) of the products **10** and 3.5 g (93% yield) **12** and check the further spectrum data analysis.

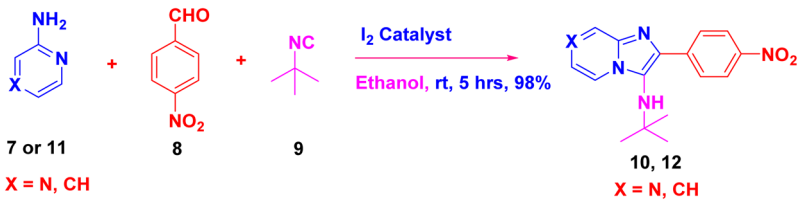

General procedure for the synthesis of 2-(4-aminophenyl)-*N*-(*tert*-butyl)imidazo [1,2-*a*]pyrazine and pyridine-3-amine (10b and 12b). **1g** of the compounds (**10a** or **12a**) was dissolved in 10 equivalent of 2.2 mL of hydrazine hydrate and it was taken in 100 RB flask, shaken vigorously to become homogeneous solution. To this reaction mixture added 0.1 equivalent (Pd/C) and refluxed the whole solution in water bath at 50 °C after 50–60 mints the reaction mixture was cooled at room temperature, filtered and then organic layer was extracted by using ethyl acetate and water, organic layer was evaporated under reduced pressure condition expected compounds (**10b**, 81 mg, 81% yield) and (**12b**, 91 mg, 91% yield) were obtained.

General procedure for the synthesis of *N*-*tert*-butyl-2-(4-nitrophenyl) imidazole[1,2-*a*] pyrazine and pyridine-3-amine (10c and 12c). 200 mg of the compounds (**10a** or **12a**) was dissolved in 9 ml of TFA and 1 ml of water, and then refluxed at 70 °C for. After 16–17 h the reaction mixture is cooled at room temperature, at which time EtOH (5 ml) is added and then reaction mixture is carefully filtered (gentle vacuum succination) using dry Celite™ filter pad, then rinsed with water. A commercial 5 N solution of NaOH (~10 ml) is added dropwise once pH 7 is reached and titration is continued until the pH 8–10 reached. The reaction mixture was cooled in ice-water bath and allow some time to form the precipitates. Finally, the total reaction mixture is isolated using suction funnel with filter paper by vacuum filtration, 2–3 times rinsed with water, dried and to affort the light brown solid products **10c** (175 mg, 86% yield) and **12c** (184 mg, 92% yield) were obtained.

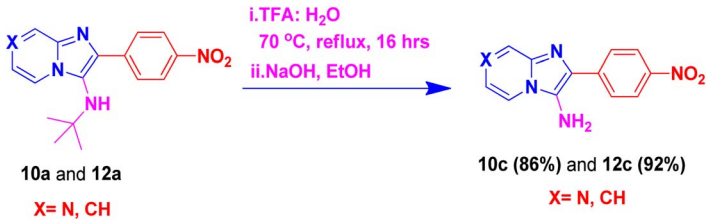

General procedure for the synthesis of 2-(4-aminophenyl) imidazo[1,2-*a*]pyrazine pyridine-3-amine (10d and 12d). 1g of the compounds (**10a** or **12a**) was dissolved in 10 equivalent of 2.2 ml of hydrazine hydrate and it was taken in 100 RB flask, shaken vigorously to become homogeneous solution. To this reaction mixture added 0.1 equivalent (Pd/C) and refluxed the whole solution in water bath at 50 °C after 50–60 minutes the reaction mixture was cooled at room temperature, filtered and then organic layer was extracted by using ethyl acetate and water, organic layer was evaporated under reduced pressure condition expected compounds **10d** (91 mg, 91% yield) and **12d** (87 mg, 87% yield) were obtained. Orange solid (3.6 g, 98%); melting point 138–140 °C; FT-IR (KBr, cm^{-1}): ν/cm 3326 (NH); ^{1}H NMR (400 MHz, $CDCl_3$; Me4Si) δ_H 9.03 (s, 1H, H-8, Py), 8.31 (d, $J = 10.1$ Hz, 4H, H-5 & H-6, Py, H-12 & H-12′, Ph), 8.14 (d, $J = 4.4$ Hz, 1H, H-11, Ph), 7.91 (d, $J = 4.5$ Hz, 1H, H-11′, Ph), 3.22 (brs, 1H, NH), 1.12 (s, 9H, Me). ^{13}C NMR (100 MHz, $CDCl_3$) δ_C 147.21 (C-13, C), 143.97 (C-8, CH), 140.82 (C-10, C), 139.57 (C-9, C), 137.59 (C-3, C), 129.29 (C-2, C), 128.71 (C-6, CH), 126.09 (C-11 & 11′, CH), 123.71 (C-12 & 12′, CH), 116.30 (C-5, CH), 57.30 (C-14, *t*-BuC), 30.50 (Me). ESI-HRMS: $C_{16}H_{17}N_5O_2$ requires 312.1460 (M + H); found 312.1465 and λ_{max} (EtOH)/nm 360.

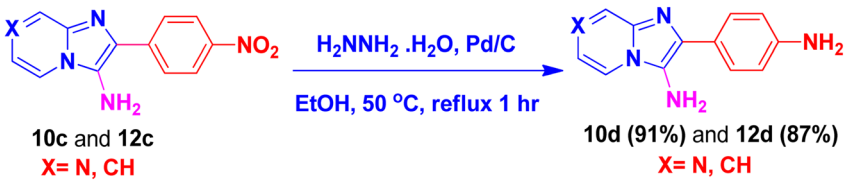

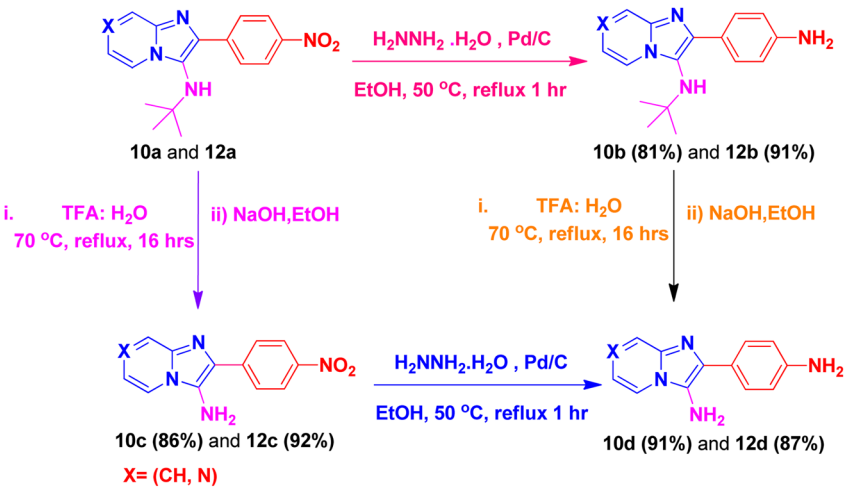

Chemical data

*N-(tert-Butyl)-2-(4-nitrophenyl)imidazo[1,2-a]pyrazin-3-amine (**10a**).*

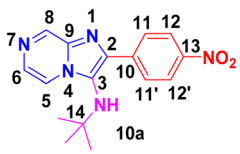

*2-(4-Aminophenyl)-N-(tert-butyl)imidazo[1,2-a]pyrazin-3-amine (**10b**).*

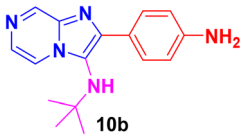

Yellowish green solid (3.0 g, 81%); HPLC purity 98%; melting point 165–167 °C; FT-IR (KBr, cm^{-1}): ν/cm 3326 (NH); ^{1}H NMR (400 MHz, DMSO-d_6) δ_H 8.80 (dd, J = 16.1, 1.3 Hz, 1H, H-8, Py), 8.41–8.29 (m, 2H, H-6 & H-5, Py), 7.99 (d, J = 8.7 Hz, 1H, H-11, Ph), 7.85 (d, J = 8.6 Hz, 1H, H-11′, Ph), 7.78 (dd, J = 9.4, 4.6 Hz, 1H, H-12, Ph), 6.87 (d, J = 8.7 Hz, 1H, H-12′, Ph), 6.59 (d, J = 8.6 Hz, 2H, NH_2), 4.61 (d, J = 28.0 Hz, 1H, NH), 0.97 (s, 9H, Me). ^{13}C NMR (100 MHz, DMSO-d_6) δ_C 152.18 (C-13, C), 148.95 (C-8, CH), 142.31(C-9, C), 142.24 (C-3, C), 141.91 (C-2, C), 129.30 (C-6, CH), 128.77 (C-11, CH), 125.81 (C-10, C), 122.29 (C-5, CH), 117.26 (C-12, CH), 56.51(C, *t*-Bu), 30.51 (Me). ESI-HRMS: $C_{16}H_{19}N_5$ requires 282.1719 (M + H); found 282.1718 and λ_{max} (EtOH)/nm 362.

*2-(4-Nitrophenyl)imidazo[1,2-a]pyrazin-3-amine (**10c**).*

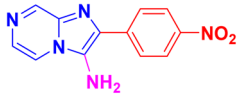

10c

Light brown solid (3.2 g, 86%); melting point 152–155 °C; FT-IR (KBr, cm-1): ν/cm 3330 (NH); ^{1}H NMR (400 MHz, DMSO-d_6) δ_H 9.40 (d, J = 1.4 Hz, 1H, H-8, Py), 8.85 (d, J = 1.4 Hz, 1H, H-5, Py), 8.58–8.48 (m, 1H, H-6, Py), 8.42–8.14 (m, 4H, Ph), 6.30 (s, 2H, NH_2). ^{13}C NMR (100 MHz, DMSO-d_6) δ_C 145.56 (C-13, C), 143.67 (C-8, CH) 143.18 (C-10, C), 141.49 (C-9, C), 134.82 (C-3, C), 131.79 (C-2, C), 128.27 (C-6, CH), 126.91 (C-11 & 11′, CH), 125.43 (C-12 & 12′, CH), 123.96 (C-5, CH). ESI-HRMS: $C_{12}H_9N_5O_2$ requires 256.0834 (M + H); found 256.0830 and λ_{max} (EtOH)/nm 425.

*2-(4-Aminophenyl)imidazo[1,2-a]pyrazin-3-amine (**10d**).*

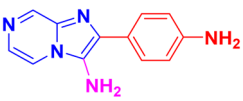

10d

Dark brown solid (2.9 g, 91%); melting point 174–177 °C; FT-IR (KBr, cm^{-1}): ν/cm 3319 (NH); ^{1}H NMR (400 MHz, DMSO-d_6) δ 9.15 (s, 1H, H-8, Py), 8.73 (d, J = 8 Hz, 1H, H-6, Py), 8.11 (d, J = 8.2 Hz, 2H, H-12 & 12′, Ph), 7.80 (d, J = 3.8 Hz, 1H, H-5, Py), 7.57 (d, J = 8.4 Hz, 2H, H-11 & 11′, Ph), 7.57 (d, J = 8.4 Hz, 2H, NH_2), 7.43 (d, J = 2.9 Hz, 2H, NH_2); ^{13}C NMR (100 MHz, DMSO-d_6) δ 137.46 (C-13, C), 136.03 (C-8, CH), 133.52 (C-9, C), 132.20 (C-3, C), 132.10 (C-2, C), 131.45 (C-6, CH), 128.92 (C-11 & 11′, CH), 124.19 (C-10, C), 118.12 (C-5, CH), 116.76 (C-12 & 12′, CH). ESI-HRMS: $C_{12}H_{11}N_5$ requires 226.1093 (M + H); found 226.1098 and λ_{max} (EtOH)/nm 376.

*N-(tert-Butyl)-2-(2-nitrophenyl)imidazo[1,2-a]pyrazin-3-amine (**10e**).*

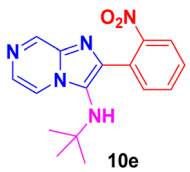

10e

Pale yellow solid (3.5 g, 93%); melting point 156–159 °C; FT-IR (KBr, cm^{-1}): ν/cm 3261 (NH); ^{1}H NMR (400 MHz, $CDCl_3$) δ_H 9.01 (d, J = 1.5 Hz, 1H, H-8, Py), 8.11 (dd, J = 4.6, 1.5 Hz, 1H, H-5, Py), 7.98 (dd, J = 8.1, 1.1 Hz, 1H, H-6, Py), 7.90 (d, J = 4.6 Hz, 1H, H-11, Ph), 7.79 (dd, J = 7.7, 1.4 Hz, 1H, H-12, Ph), 7.70 (td, J = 7.6, 1.3 Hz, 1H, H-12′, Ph), 7.56 (ddd, J = 8.1, 7.5, 1.5 Hz, 1H, H-13, Ph), 2.83 (sbr, 1H, NH), 0.97 (s, 9H, Me). ^{13}C NMR (100 MHz, $CDCl_3$) δ_C 149.35 (C-11, C), 143.86 (C-8, CH), 139.48 (C-9, C), 138.96 (C-3, C), 137.58 (C-12′, CH), 132.77 (C-2, C), 132.76 (C-11′, CH), 129.29 (C-6, CH), 129.18 (C-13, CH), 126.50 (C-12, CH), 126.12 (C-5, CH), 116.21 (C-10, C), 56.12 (*t*-Bu C), 30.10 (Me). ESI-HRMS: $C_{16}H_{17}N_5O_2$ 312.1460 (M + H); found 312.1462 and λ_{max} (EtOH)/nm 360.

*2-(2-Aminophenyl)-N-(tert-Butyl)imidazo[1,2-a]pyrazin-3-amine (**10f**).*

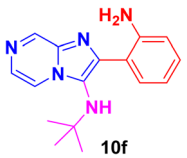

10f

Greenish yellow solid (3.2 g, 90%); melting point 167–169 °C; FT-IR (KBr, cm^{-1}): ν/cm 3360 (NH); ^{1}H NMR (400 MHz, $CDCl_3$) δ_H 8.97 (d, J = 1.4 Hz, 1H, H-8, Py), 8.16 (dd, J = 4.6, 1.4 Hz, 1H, H-5, Py), 7.85 (d, J = 4.6 Hz, 1H, H-6, Py), 7.47 (dd, J = 7.6, 1.5 Hz, 1H, H-11′, Ph), 7.27 (s, 1H, H-13, Ph), 7.19 (td, J = 8.0, 1.5 Hz, 1H, H-12, Ph), 6.82 (dd, J = 8.0, 0.8 Hz, 2H, H-12′, NH_2), 0.97 (d, J = 3.1 Hz, 9H, Me), ^{13}C NMR (101 MHz, $CDCl_3$) δ_C 144.72 (C-11, C), 143.93 (C-8, CH), 137.42 (C-9, C), 132.70 (C-3, C), 130.43 (C-2, C), 129.47 (C-6, CH), 128.82 (C-5, CH), 126.26 (C-13, CH), 124.13 (C-11′, CH), 118.72 (C-12′, CH), 116.68 (C-12, CH), 116.29 (C-10, C), 57.13 (*t*-BuC), 29.38 (Me). ESI-HRMS: $C_{16}H_{19}N_5$ requires 282.1719 (M + H); found 282.1715 and λ_{max} (EtOH)/nm 362.

*2-(2-Aminophenyl)imidazo[1,2-a]pyrazin-3-amine (**10g**).*

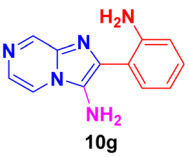

10g

Dark brown solid (2.7 g, 84%); melting point 176–179 °C; FT-IR (KBr, cm^{-1}): ν/cm 3299 (NH); 1H NMR (400 MHz, DMSO-d_6) δ_H 8.79 (d, J = 9.9 Hz, 1H, H-11′, Ph), 8.34 (t, J = 5.5 Hz, 1H, H-8, Py), 7.90 (dd, J = 20.5, 7.9 Hz, 1H, H-5, Py), 7.75(dd, J = 4.6, 2.2 Hz, 1H, H-6, Py), 7.57 (t, J = 8.2 Hz, 1H, H-13, Ph), 6.79 (d, J = 7.9 Hz, 1H, H-12, Ph), 6.65 (t, J = 7.4 Hz, 1H, H-12′, Ph), 6.04 (s, 2H, NH_2), 5.69 (s, 2H, NH_2). ^{13}C NMR (101 MHz, DMSO-d_6) δ_C 149.23 (C-11, C), 146.91 (C-8, CH), 143.01 (C-9, C), 141.75 (C-3, C), 132.80 (C-2, C), 131.33 (C-6, CH), 129.19 (C-13, CH), 128.77 (C-11′, CH), 128.54 (C-5, CH), 128.39 (C-12, CH), 124.71 (C-12′, CH), 116.46 (C-10, C). ESI-HRMS: $C_{12}H_{11}N_5$ requires 226.1093 (M + H); found 226.1095 and λ_{max} (EtOH)/nm 384.

*N-(tert-Butyl)-2-(4-(dimethylamino)phenyl)imidazo[1,2-a] pyrazin-3-amine (**10h**).*

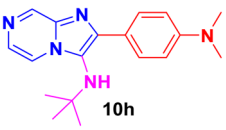

10h

Yellow solid (3.3 g, 90%); melting point 205–207 °C; FT-IR (KBr, cm^{-1}):ν/cm 3257 (NH); ^{1}H NMR (400 MHz, $CDCl_3$) δ_H 8.95 (d, J = 6.9 Hz, 1H, H-8, Py), 8.11 (dd, J = 4.0, 4.0 Hz, 1H, H-6, Py), 7.82–7.81 (m, 3H, H-5, Py & H-11, H-11′, Ph), 6.80 (d, J = 9.0 Hz, 2H, H-12 & 12′, Ph), 3.02 (s, 6H, $N(Me)_2$), 2.07 (br s, 1H, NH), 1.08 (s, 9H, Me). ^{13}C NMR (101 MHz, $CDCl_3$) δ_C 150.23 (C-13, C), 142.29 (C-8, CH), 142.61 (C-9, C), 137.18 (C-3, C), 129.02 (C-2, C), 128.68 (C-6, CH), 123.99 (C-11 & 11′, CH), 121.92 (C-10, C), 116.2 (C-5, CH), 112.03 (C-12 & 12′, CH), 56.85 (*t*-BuC), 40.36 ($N(Me)_2$), 30.42 (Me). ESI-HRMS: $C_{16}H_{23}N_5$ requires 310.2032 (M + H); found 310.2036 and λ_{max} (EtOH)/nm 370.

2-(4-(Dimethylamino)phenyl)imidazo[1,2-a]pyrazin-3-amine ***(10i)***.

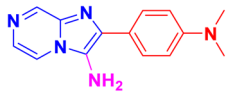

10i

Pale Yellow solid (2.9 g, 87%); melting point 210–213 °C; FT-IR (KBr, cm^{-1}): ν/cm 3312 (NH); ^{1}H NMR (400 MHz, DMSO-d_6) δ_H 8.88 (s, 1H, H-8, Py), 8.33 (dd, J = 17.5, 5.9 Hz, 1H, H-5, Py), 7.88 (d, J = 4.5 Hz, 3H, H-6, Py & H-11 & H-11′, Ph), 7.74–7.72 (m, 2H, H-12 & H-12′, Ph), 6.83 (d, J = 8.6 Hz, 2H, NH_2), 2.98 (s, 6H, $N(Me)_2$); ^{13}C NMR (101 MHz, DMSO-d_6) δ_C 151.16 (C-13, C), 140.34 (C-8. CH), 134.74 (C-9, C), 132.37 (C-3, C), 129.85 (C-2, C), 128.78 (C-6, CH), 119.46 (C-11 & C-11′, CH), 119.29 (C-10, C), 112.47 (C-12 & 12′, CH), 39.36 ($N(Me)_2$); ESI-HRMS: $C_{14}H_{15}N_5$ requires 254.1406 (M + H); found 254.1408 and λ_{max} (EtOH)/nm 368.

N-Cyclohexyl-2-(4-nitrophenyl)imidazo[1,2-a]pyrazin-3-amine ***(10j)***.

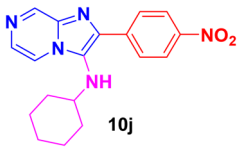

10j

Yellowish brown solid (3.6 g, 97%); melting point 154–156 °C; FT-IR (KBr, cm^{-1}): ν/cm 3249 (NH); ^{1}H NMR (400 MHz, $CDCl_3$) δ_H 9.02 (s, 1H, H-8, Py), 8.32 (s, 4H, H-5 & 6, Py, H-12 & H-12′, Ph), 7.94 (dd, J = 38.3, 4.0 Hz, 2H, H-11 & H-11′, Ph), 3.21 (br s, 1H, NH), 3.01 (s, 1H, aliphatic CH), 1.81–1.60 (m, 5H, CH_2), 1.30–1.12 (m, 5H, CH_2). ^{13}C NMR (101 MHz, $CDCl_3$) δ_C 147.16 (C-13, C), 144.15 (C-10, C), 140.12 (C-8, CH), 137.12 (C-3, C), 136.48 (C-2, C), 129.40 (C-6, CH), 127.68 (C-11, CH), 127.54 (C-11′, CH), 123.98 (C-12 & 12′, CH), 115.51 (C-5, CH), 57.22 (aliphatic CH), 34.43 (CH_2), 25.47 (CH_2), 24.78 (CH_2). ESI-HRMS: $C_{18}H_{19}N_5O_2$ requires 338.1617 (M + H); found 338.1615 and λ_{max} (EtOH)/nm 364.

2-(4-Aminophenyl)-N-cyclohexylimidazo[1,2-a]pyrazin-3-amine ***(10k)***.

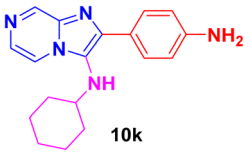

10k

Yellowish brown solid (3.4 g, 94%); melting point 172–175 °C; FT-IR (KBr, cm^{-1}): ν/cm 3249 (NH); ^{1}H NMR (400 MHz, $CDCl_3$) δ_H 8.93 (d, J = 1.4 Hz, 1H, H-8, Py), 7.98 (dd, J = 4.6, 1.4 Hz, 1H, H-5, Py), 7.82 (dd, J = 5.6, 2.9 Hz, 3H, H-6, Py, H-11 & H-11′, Ph), 6.80–6.66 (m, 2H, H-12 & H-12′, Ph), 6.50 (s, 2H, NH_2), 3.21 (br s, 1H, NH), 3.01 (s, 1H, aliphatic CH), 1.75 (dd, J = 42.2, 7.9 Hz, 6H, CH_2), 1.28–1.06 (m, 4H, CH_2). ^{13}C NMR (101 MHz, $CDCl_3$) δ_C 146.165 (C-13, C), 144.25 (C-8, CH), 141.16 (C-3, C), 136.61 (C-2, C), 128.79 (C-6, CH), 128.49 (C-11 & C-13′, CH), 125.39 (C-10, C), 123.75 (C-5, CH), 115.51 (C-12 & C-12′, CH), 56.77 (aliphatic CH), 34.28 (CH_2), 29.69 (CH_2), 25.63 (CH_2), 24.79 (CH_2). ESI-HRMS: $C_{18}H_{21}N_5$ requires 308.1875 (M + H); found 308.1878 and λ_{max} (EtOH)/nm 390.

2-(2-Nitrophenyl)imidazo[1,2-a]pyrazin-3-amine ***(10l)***.

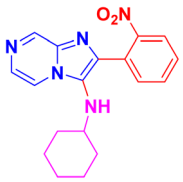

10l

Dark brown solid (3.2 g, 86%); melting point 159–161 °C; FT-IR (KBr, cm^{-1}): ν/cm 3208 (NH); ^{1}H NMR (400 MHz, $CDCl_3$) ^{1}H NMR (400 MHz, $CDCl_3$) δ_H 8.77 (s, 1H, H-8, Py), 8.10 (s, 2H, H-5 & 6, Py), 7.79 (dd, J = 67.9, 41.3 Hz, 4H, H-11, H-12, H-12′ & H-13, Ph), 3.69 (br s, 1H, NH), 2.72 (s, 1H, aliphatic CH), 1.68–1.38 (m, 6H, CH_2), 1.19–0.71 (m, 4H, CH_2). ^{13}C NMR (101 MHz, $CDCl_3$) δ_C 148.19 (C-11, C), 136.98 (C-8, CH), 134.11 (C-9, C), 133.62 (C-3, C), 132.37 (C-12′, CH), 131.38 (C-2, C), 127.86 (C-11′, CH), 125.39 (C-6, CH), 125.14 (C-13, CH), 122.65 (C-10, C), 121.46 (C-12, CH), 116.72 (C-5, CH), 56.43 (aliphatic CH), 33.52(CH_2), 25.26 (CH_2), 24.48 (CH_2). ESI-HRMS: $C_{16}H_{17}N_5O_2$ requires 338.1617 (M + H); found 338.1614 and λ_{max} (EtOH)/nm 390.

2-(2-Aminophenyl)-N-cyclohexylimidazo[1,2-a]pyrazin-3-amine ***(10m)***.

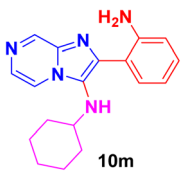

10m

Dark brown solid (2.6 g, 80%); melting point 178–181 °C; FT-IR (KBr, cm^{-1}): ν/cm 3299 (NH); ^{1}H NMR (400 MHz, $CDCl_3$) δ_H 8.12 (dd, J = 6.8, 1.2 Hz, 1H, H-11′, Ph), 7.56–7.49 (m, 2H, H-8 & H-5, Py), 7.31 (d, J = 2.4 Hz, 1H, H-6, Py), 7.19–7.12 (m, 2H, H-13 & H-12, Ph), 6.86–6.77 (m, 3H, H-12′, Ph, NH_2), 3.69 (br s, NH), 2.12 (s, 1H, aliphatic CH), 1.65 (dd, J = 71.4, 23.8 Hz, 6H, CH_2), 1.12 (d, J = 7.3 Hz, 4H, CH_2). ^{13}C NMR (101 MHz, $CDCl_3$) δ_C 145.14 (C-11, C), 141.15 (C-8, CH), 135.01 (C-9, C), 129.59 (C-3, C), 128.57 (C-2, C), 125.78 (C-6, CH), 123.72 (C-13, CH), 122.53 (C-11′, CH), 119.25 (C-5, CH), 118.18 (C-12, CH), 116.88 (C-12′, CH), 116.51 (C-10, C), 56.01 (aliphatic CH), 33.91 (CH_2), 25.64 (CH_2), 24.73 (CH_2). ESI-HRMS: $C_{18}H_{21}N_5$ requires 308.1875 (M + H); found 308.1870 and λ_{max} (EtOH)/nm 384.

N-(tert-Butyl)-2-(4-nitrophenyl)imidazo[1,2-a]pyridin-3-amine ***(12a)***.

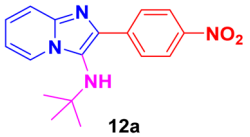

12a

Yellowish brown solid (3.5 g, 93%); melting point 140–142 °C; FT-IR (KBr, cm^{-1}): ν/cm 3350 (NH); ^{1}H NMR (400 MHz, $CDCl_3$) δ_H 8.25 (s, 4H, H-12 & H-12′, H-11 & H-12′, Ph), 8.18 (d, J = 6.9 Hz, 1H, H-5, Py), 7.55 (d, J = 9.0 Hz, 1H, H-8, Py), 7.23–7.15 (m, 1H, H-7, Py), 6.82 (t, J = 6.8 Hz, 1H, H-6, Py), 3.08 (br s, 1H, NH), 1.09 (s, 9H, Me). ^{13}C NMR (101 MHz, $CDCl_3$) δ_C 146.62 (C-13, C), 142.54 (C-9, C), 141.99 (C-10, C), 137.08 (C-3, C), 128.39 (C-2, C), 125.01 (C-7, CH), 123.54 (C-5, CH), 123.41 (C-11 & C-11′, CH), 117.70 (C-12 & C-12′, CH), 114.56 (112.02, C-8, CH), (C-6, CH), 56.79 (aliphatic CH), 30.48 (Me). ESI-HRMS: $C_{16}H_{17}N_5O_2$ requires 311.1508 (M + H); found 311.1500 and λ_{max} (EtOH)/nm 368.

2-(4-Aminophenyl)-N-(tert-butyl)imidazo[1,2-a]pyridin-3-amine ***(12b)***.

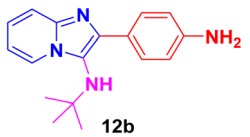

12b

Pale yellowish brown solid (3.2 g, 91%); HPLC purity 98%; melting point 160–163 °C; FT-IR (KBr, cm^{-1}): ν/cm 3258 (NH); ^{1}H NMR (400 MHz, DMSO-d_6) δ_H 8.42 (d, J = 6.9 Hz, 1H, H-5, Py), 7.73 (dd, J = 7.7, 1.3 Hz, 2H, H-11 & H-11′, Ph), 7.47 (d, J = 9.1 Hz, 1H, H-8, Py), 7.24–7.16 (m, 1H, H-7, Py), 7.09–6.72 (m, 3H, H-12 & H-12′, Ph, H-6, Py) 3.26 (brs, 3H, NH, NH_2), 0.93 (s, 9H, Me). ^{13}C NMR (101 MHz, DMSO-d_6) δ_C 146.86 (C-13, C), 141.08 (C-9, C), 130.90 (C-3, C), 128.50 (C-2, C), 124.18 (C-11 & C-11′, CH), 124.12 (C-7, CH), 124.09 (C-5, CH), 119.78 (C-12 & C-12′, CH), 116.77 (C-6, CH), 116.20 (C-8, CH), 56.04 (aliphatic CH), 30.31 (Me). ESI-HRMS: $C_{17}H_{20}N_4$ requires 281.1766 (M + H); found 281.1760 and λ_{max} (EtOH)/nm 360.

2-(4-Nitrophenyl)imidazo[1,2-a]pyridin-3-amine ***(12c)***.

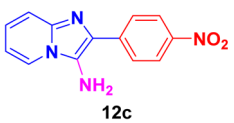

12c

Light brown solid (3.2 g, 92%); melting point 154–156 °C; FT-IR (KBr, cm^{-1}): ν/cm 3208 (NH); ^{1}H NMR (400 MHz, DMSO-d_6) δ_H 8.86 (d, J = 29.0 Hz, 1H, H-5, Py), 8.22 (d, J = 7.3 Hz, 1H, H-12, Ph), 8.00 (t, J = 11.1 Hz, 1H, H-12′, Ph), 7.96–7.85 (m, 2H, H-11 & H-11′, Ph), 7.69 (d, J = 7.6 Hz, 1H, H-8, Py), 7.47 (t, J = 9.2 Hz, 2H, H-7 & H-6, Py), 6.57 (s, 2H, NH_2). ^{13}C NMR (101 MHz, DMSO-d_6) δ_C 157.71 (C-13, C), 157.33 (C-9, C), 147.22 (C-10, C), 143.21 (C-3, C), 139.36 (C-2, C), 127.85 (C-12 & C-12′, CH), 127.59 (C-7, CH), 124.48 (C-5, CH), 117.52 (C-11 & C-11′, CH), 114.75 (C-6, CH), 114.15 (C-8, CH), ESI-HRMS: $C_{13}H_{10}N_4O_2$ requires 255.0800 (M + H); found 255.0807 and λ_{max} (EtOH)/nm 332.

2-(4-Aminophenyl)imidazo[1,2-a]pyridin-3-amine ***(12d)***.

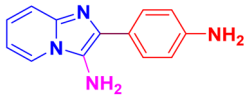

12d

Dark brown solid (2.8 g, 87%); melting point 170–172 °C; FT-IR (KBr, cm^{-1}): ν/cm 3400 (NH); ^{1}H NMR (400 MHz, DMSO-d_6) δ_H 8.86 (d, J = 29.0 Hz, 1H, H-8, Py), 8.22 (d, J = 7.3 Hz, 1H, H-5, Py), 8.00 (t, J = 11.1 Hz, 2H, H-6 & H-7, Py), 7.96–7.85 (m, 2H, H-11 & H-11′, Ph), 7.69 (d, J = 7.6 Hz, 2H, H-12 & H-12′, Ph), 7.01 (t, J = 9.2 Hz, 2H, NH_2), 6.99–6.57 (d, J = 8.4 Hz, 2H, NH_2). ^{13}C NMR (101 MHz, DMSO-d_6) δ_C 144.46 (C-13, C), 136.11 (C-9, C), 135.72 (C-3, C), 135.27 (C-2, C), 131.72 (C-11 & C-11′, CH), 128.13 (C-7, CH), 125.11 (C-7, CH), 116.51 (C-5, CH), 113.92(C-10, C), 112.52 (C-12 & C-12′, CH), 112.05 (C-6, CH). ESI-HRMS: $C_{13}H_{12}N_4$ requires 225.1140 (M + H); found 225.1146 and λ_{max} (EtOH)/nm 314.

N-(tert-Butyl)-2-(2-nitrophenyl)imidazo[1,2-a]pyridin-3-amine ***(12e)***.

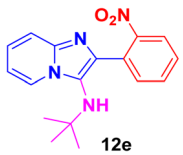

12e

Dark Reddish brown solid (3.5 g, 94%); melting point 156–159 °C; FT-IR (KBr, cm^{-1}): ν/cm 3249 (NH); ^{1}H NMR (400 MHz, $CDCl_3$) δ_H 8.19 (d, J = 6.9 Hz, 1H, H-5, Py), 7.91 (dd, J = 8.1, 0.7 Hz, 1H, H-11′, Ph), 7.81 (dd, J = 7.7, 1.4 Hz, 1H, H-12, Ph), 7.66 (t, J = 7.6 Hz, 1H, C-12′, Ph), 7.57–7.47 (m, 2H, H-13 & H-8, Py), 7.21–7.13 (m, 1H, H-7, Py), 6.81 (t, J = 6.8 Hz, 1H, H-6, Py), 2.74 (br s, 1H, NH), 0.92 (s, 9H, Me). ^{13}C NMR (101 MHz, $CDCl_3$) δ_C 149.47 (C-11, C), 142.42 (C-9, C), 136.17 (C-3, C), 132.83 (C-2, C), 132.43 (C-12′, CH), 130.27 (C-11′, CH), 128.40 (C-13, CH), 124.68 (C-10, C), 124.27 (C-7, CH), 123.34 (C-5, CH), 117.70 (C-8, CH), 111.80 (C-6, CH), 55.63 (*t*-Bu C), 30.05 (Me). ESI-HRMS: $C_{17}H_{18}N_4O_2$ requires 311.1508 (M + H); found 311.1505 and λ_{max} (EtOH)/nm 396.

2-(2-Aminophenyl)-N-(tert-butyl)imidazo[1,2-a]pyridin-3-amine ***(12f)***.

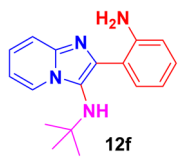

12f

Pale brown solid (2.8 g, 80%); melting point 176–179 °C; FT-IR (KBr, cm^{-1}): ν/cm 3258 (NH); ^{1}H NMR (400 MHz, DMSO-d_6) δ_H 8.42 (d, J = 6.9 Hz, 1H, H-11′, Ph), 7.73 (dd, J = 7.7, 1.3 Hz, 1H, H-5, Py), 7.47 (d, J = 9.1 Hz, 1H, H-8, Py), 7.24–7.16 (m, 1H, H-13, Ph), 6.90 (d, J = 6.6 Hz, 2H, H-7 & H-6, Py), 6.74 (d, J = 7.4 Hz, 1H, H-12′, Ph), 6.61 (d, J = 6.2 Hz, 1H, H-12, Ph), 4.60 (s, 2H, NH_2), 3.25(s br NH), 0.93 (s, 9H, Me). ^{13}C NMR (101 MHz, DMSO-d_6) δ_C 146.86 (C-11, C), 141.08 (C-9, C), 130.90 (C-3, C), 128.50 (C-2, C), 124.18 (C-5, CH), 124.12 (C-7, CH), 124.09 (C-5,

CH), 119.78 (C-11′, CH), 116.77 (C-12 & C-12′, CH), 116.20 (C-6, CH), 116.10 (C-8, CH), 111.46 (C-10, C), 56.04 (*t*-Bu C), 32.01 (Me). ESI-HRMS: $C_{17}H_{20}N_4$ requires 281.1760 (M + H); found 281.1764 and λ_{max} (EtOH)/nm 362.

*2-(2-Nitrophenyl)imidazo[1,2-a]pyridin-3-amine (**12g**).*

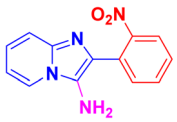

12g

Dark brown solid (3.0 g, 85%); melting point 164–167 °C; FT-IR (KBr, cm^{-1}): ν/cm 3330 (NH); ^{1}H NMR (400 MHz, DMSO-d_6) δ_H 8.42 (d, J = 6.9 Hz, 1H, H-5, Py), 7.73 (dd, J = 7.7, 1.3 Hz, 1H, H-11′, Ph), 7.47 (d, J = 9.1 Hz, 1H, H-12, Ph), 7.21 (dd, J = 16.9, 2.4 Hz, 2H, H-12′ & H-13, Ph), 7.01 (d, J = 7.0 Hz, 1H, H-8, Py), 6.90 (d, J = 6.6 Hz, 1H, H-7, Py), 6.74 (d, J = 7.4 Hz, 1H, H-6, Py), 6.61 (br s, 1H, NH_2). ^{13}C NMR (101 MHz, DMSO-d_6) δ_C 148.10 (C-11′, C), 135.34 (C-9, C), 134.72 (C-3, C), 134.14 (C-2, C), 131.53 (C-12′, CH), 131.38 (C-11′, CH), 130.35 (C-13, CH), 125.98 (C-7, CH), 125.17 (C-5, CH), 122.50 (C-10, C), 116.31 (C-12, CH), 112.43 (C-8, CH), 111.39 (C-6, CH). ESI-HRMS: $C_{13}H_{10}N_4O_2$ requires 255.0882 (M + H); found 255.0888 and λ_{max} (EtOH)/nm 363.

*2-(2-Aminophenyl)imidazo[1,2-a]pyridin-3-amine (**12h**).*

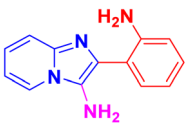

12h

Dark reddish brown solid (2.5 g, 83%); melting point 179–181 °C; FT-IR (KBr, cm^{-1}): ν/cm 3336 (NH); ^{1}H NMR (400 MHz, DMSO-d_6) δ_H 8.50 (d, J = 6.8 Hz, 1H, C-11′, Ph), 8.23 (d, J = 7.1 Hz, 1H, H-5, Py), 7.94 (d, J = 9.0 Hz, 1H, H-8, Py), 7.80 (d, J = 7.4 Hz, 1H, H-13, Ph), 7.61 (s, 1H, H-7, Py), 7.38–7.31 (m, 2H, H-12′ & H-12, Ph), 7.17 (dd, J = 17.8, 9.3 Hz, 1H, H-6, Py), 7.07–6.99 (m, 2H, NH_2), 3.40 (s, NH_2). ^{13}C NMR (101 MHz, DMSO-d_6) δ_C 143.93 (C-11′, C), 141.94 (C-9, C), 130.35 (C-3, C), 129.84 (C-2, C), 125.88 (C-13, CH), 125.55 (C-5, CH), 125.32 (C-7, CH), 124.47 (C-11′, CH), 122.48 (C-12, CH), 120.93 (C-12′, CH), 120.54 (C-6, CH), 115.20 (C-8, CH), 110.56 (C-10, C). ESI-HRMS: $C_{13}H_{12}N_4$ requires 225.1140 (M + H); found 225.1145 and λ_{max} (EtOH)/nm 366.

*N-(tert-Butyl)-2-(4-(dimethylamino)phenyl)imidazo[1,2-a] pyridin-3-amine (**12i**).*

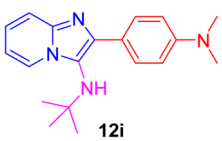

12i

White solid (3.4 g, 92%); melting point 206–208 °C; FT-IR (KBr, cm^{-1}): ν/cm 3280 (NH); ^{1}H NMR (400 MHz, $CDCl_3$) δ_H 8.23 (d, J = 6.9 Hz, 1H, H-5, Py), 7.87–7.81 (m, 2H, H-11 & H-11′, Ph), 7.56 (d, J = 9.0 Hz, 1H, H-7, Py), 7.13 (ddd, J = 8.9, 6.7, 1.3 Hz, 1H, H-8, Py), 6.83–6.74 (m, 3H, H-6, Py, H-12 & H-12′, Ph), 3.41 (br s, 1H, NH), 3.02 (s, 6H, $N(Me)_2$), 1.08 (s, 9H, Me). ^{13}C NMR (101 MHz, $CDCl_3$) δ_C 149.87 (C-13, C), 141.67 (C-9, C), 139.52 (C-3, C), 128.96 (C-2, C), 123.91 (C-11 & C-11′, CH), 123.38 (C-5, CH), 122.25 (C-7, CH), 116.72 (C-10, C), 112.15 (C-6, CH), 111.21 (C-8, CH), (C-12 & C-12′, CH), 56.37 (*t*-Bu C), 40.52 ($N(Me)_2$), 30.43 (Me). ESI-HRMS: $C_{19}H_{24}N_4$ requires 309.2079 (M + H); found 309.2070 and λ_{max} (EtOH)/nm 358.

*2-(4-(Dimethylamino)phenyl)imidazo[1,2-a]pyridin-3-amine (**12j**).*

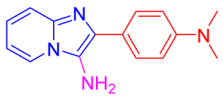

12j

Pale white solid (3.0 g, 88%); melting point 214–217 °C; FT-IR (KBr, cm^{-1}): ν/cm 3385 (NH); ^{1}H NMR (400 MHz, DMSO-d_6) δ_H 8.18 (d, J = 6.7 Hz, 1H, H-5, Py), 7.75 (d, J = 8.7 Hz, 2H, H-11 & H-11′, Ph), 7.61 (d, J = 9.0 Hz, 1H, H-8, Py), 7.39–7.31 (m, 1H, H-7, Py), 6.99 (t, J = 6.6 Hz, 1H, H-6, Py), 6.81 (d, J = 8.8 Hz, 2H, H-12 & H-12′, Ph), 3.45 (br s, NH_2), 2.95 (s, 6H, $N(Me)_2$). ^{13}C NMR (101 MHz, DMSO-d_6) δ_C 157.75 (C-13, C), 157.11 (C-9, C), 150.62 (C-3, C), 141.78 (C-2, C), 127.89 (C-11 & C-11′, CH), 125.88 (C-5, CH), 123.90 (C-7, CH), 120.66 (C-10, C), 116.87(C-8, CH), 112.88 (C-6, CH), 112.54 (C-12 & C-12′, CH), 31.04 ($N(Me)_2$). ESI-HRMS: $C_{15}H_{16}N_4$ requires 253.1453 (M + H); found 253.1456 and λ_{max} (EtOH)/nm 358.

*N-Cyclohexyl-2-(4-nitrophenyl)imidazo[1,2-a]pyridin-3-amine (**12k**).*

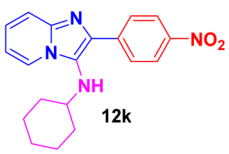

12k

Orange solid (3.3 g, 90%); melting point 237–240 °C; FT-IR (KBr, cm^{-1}): ν/cm 3290 (NH); ^{1}H NMR (400 MHz, $CDCl_3$) δ_H 8.32 (dd, J = 9.1, 4.2 Hz, 1H, H-5, Py), 8.05 (d, J = 6.9 Hz, 2H, H-12 & H-12′, Ph), 7.54 (d, J = 9.1 Hz, 2H, H-11 & H-11′, Ph), 7.22–7.14 (m, 2H, H-8 & H-7, Py), 6.83 (d, J = 6.7 Hz, 1H, H-6, Py), 3.11 (s br, 1H, NH), 2.97 (td, J = 10.0, 5.6 Hz, 1H, aliphatic CH), 2.16 (s, 2H, CH_2), 1.88–1.54 (m, 4H, CH_2), 1.22 (dt, J = 18.4, 9.5 Hz, 4H, CH_2). ^{13}C NMR (101 MHz, $CDCl_3$) δ_C 146.50 (C-13, C), 142.09 (C-9, C), 141.19 (C-10, C), 134.41 (C-3, C), 127.23 (C-2, C), 126.55 (C-11 & C-11′, CH), 124.86 (C-5, CH), 123.78 (C-7, CH), 122.70 (C-12 & C-12′, CH), 117.85 (C-6, CH), 112.23 (C-8, CH), 57.08 (aliphatic CH), 34.30 (CH_2), 25.61 (CH_2), 24.82 (CH_2). ESI-HRMS: $C_{19}H_{20}N_4O_2$ requires 337.1665 (M + H); found 337.1668 and λ_{max} (EtOH)/nm 370.

*2-(4-Aminophenyl)-N-cyclohexylimidazo[1,2-a]pyridin-3-amine (**12l**).*

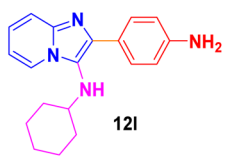

12l

Reddish brown solid (2.8 g, 84%); melting point 248–251 °C; FT-IR (KBr, cm^{-1}): ν/cm 3350 (NH); ^{1}H NMR (400 MHz, $CDCl_3$) δ_H

8.09 (d, $J = 6.7$ Hz, 1H, H-5, Py), 7.92 (d, $J = 8.3$ Hz, 1H, H-8, Py), 7.84 (d, $J = 8.3$ Hz, 2H, H-11 & H-12′, Ph), 7.50 (d, $J = 8.8$ Hz, 1H, H-7, Py), 7.08 (d, $J = 8.1$ Hz, 1H, H-6, Py), 6.77 (d, $J = 7.1$ Hz, 2H, H-11 & H-11′, Ph), 3.81 (sbr, 2H, NH_2), 3.10 (dd, $J = 13.6$, 4.3, 1H, NH), 3.07–2.95 (m, 1H, aliphatic CH), 1.71 (dd, $J = 71.0$, 25.7 Hz, 5H), 1.19 (dt = J 18.9, 9.0 Hz, 5H, CH_2) ^{13}C NMR (101 MHz, $CDCl_3$) δ_C 145.68 (C-13, C), 141.33 (C-9, C), 137.17 (C-3, C), 128.19 (C-2, C), 127.75 (C-11 & C-11′, CH), 124.96 (C-10, C), 123.45 (C-5, CH), 122.80 (C-7, CH), 115.10 (C-6, CH), 114.06 (C-8, CH), 111.24 (C-12 & C-12′, CH), 56.82 (aliphatic CH), 34.15 (CH_2), 25.76 (CH_2), 24.82 (CH_2). ESI-HRMS: $C_{19}H_{22}N_4$ requires 307.1923 (M + H); found 307.1928 and λ_{max} (EtOH)/nm 348.

Author contributions

A. P.: supervision, formal analysis, original draft-review & editing. R. K.: conceptualization, methodology, formal analysis, writing.

Conflicts of interest

The authors declare that there are no conflicts of interest.

Acknowledgements

The authors heartily thank to Dr S. Thennarasu, Chief Scientist and Head, CSIR-Central Leather Research Institute (CSIR-CLRI), Adyar, Chennai, Tamilnadu-600020, India for providing research support and Central Instrumentation Facilities (CIF) for characterizing the compounds. We heartfelt thank to Prof. USN Murty, Director of the National Institute of Pharmaceutical Education and Research Guwahati (NIPER-G) for excellent support. Authors also thankful to Department of Biotechnology under the Centre of GMP extraction facility for necessary support.

References

1 C. B. Blackadar, *World J. Clin. Oncol.*, 2016, **7**, 54–86.
2 P. S. Roy and B. J. Saikia, *Indian J. Cancer*, 2016, **53**, 441–442.
3 W. Report, *WHO Cancer Report*, 2019.
4 S. Srivastava, E. J. Koay, A. D. Borowsky, A. M. Marzo, S. Ghosh, P. D. Wagner and B. S. Kramer, *Nat. Rev. Cancer*, 2019, **19**, 349–358.
5 (*a*) A. Domling, *Chem. Rev.*, 2006, **106**, 17–89; (*b*) H. S. P. Rao and A. Parthiban, *Org. Biomol. Chem.*, 2014, **12**, 6223–6238; (*c*) A. Parthiban and P. Makam, *RSC Adv.*, 2022, **12**, 29253–29290.
6 (*a*) Y. Tanaka, T. Hasui and M. Suginome, *Org. Lett.*, 2007, **9**, 4407–4410; (*b*) L. EI Kaim, L. Grimaud and J. Oble, *Angew. Chem., Int. Ed.*, 2005, **44**, 7961–7964; (*c*) P. R. Andreana, C. C. Liu and S. L. Schreiber, *Org. Lett.*, 2004, **6**, 4231–4233.
7 (*a*) N. M. Shukla, D. B. Salunke, E. Yoo, C. A. Mutz, R. Balakrishna and S. A. Davi, *Bioorg. Med. Chem.*, 2012, **20**, 5850–5863; (*b*) M. H. Fischer and A. Lusi, *J. Med. Chem.*, 1972, **15**, 982–985.
8 M. H. Fischer and A. Lusi, *J. Med. Chem.*, 1972, **15**, 982–985.
9 K. S. Gudmundsson, J. D. Williams, J. C. Drach and L. B. Townsend, *J. Med. Chem.*, 2003, **46**, 1449–1455.
10 C. Hamdouchi, J. D. Blas, M. Del Prado, J. Gruber, B. A. Heinz and L. Vance, *J. Med. Chem.*, 1999, **42**, 50–53.
11 M. Lhassani, O. Chavignon, J. M. Chezal, J. C. Teulade, J. P. Chapat, R. Snoeck, G. Andrei, J. Balzarini, E. D. Clercq and A. Gueiffer, *Eur. J. Med. Chem.*, 1999, **34**, 271–275.
12 J. B. Veron, H. Allouchi, C. Enguedhar Gueiffier, R. Snoeck, G. Andrei, E. D. Clercq and A. Gueiffier, *Bioorg. Med. Chem.*, 2008, **16**, 9536–9545.
13 (*a*) L. Almirante, L. Polo, A. Mugnaini, E. Provinciali, P. Rugarli, A. Biancotti, A. Gamba and W. Murmann, *J. Med. Chem.*, 1965, **8**, 305–312; (*b*) Y. K. M. Flores, M. E. C. Aldrete, H. S. Zamora, J. C. Basurto and M. Camargo, *Med. Chem. Res.*, 2012, **21**, 775–782.
14 M. G. Rimoli, L. Avallone, P. Caprariis, E. Luraschi, W. Filippelli, L. Berrino and F. Rossi, *Eur. J. Med. Chem.*, 1997, **32**, 195–203.
15 M. J. Mulvihill, J. Qun Sheng, H. R. Coate, A. Cooke, H. Dong, L. Feng, K. Foreman, R. F. Maryland, A. Honda, G. Mak, K. M. Mulvihill, A. I. Nigro, M. O. Connor, C. Pirrit, A. G. Steinig, S. Kam, K. M. Stolz, S. Yingchuan, P. A. R. Tavares, Y. Yao and N. W. Gibson, *Bioorg. Med. Chem.*, 2008, **16**, 1359–1375.
16 S. M. Gonzalez, A. I. Hernandez, C. Varela, R. A. Sonsoles, R. M. Alvarez, A. B. Garcia, M. Lorenzo, M. Rivero, J. Oyarzabal, R. Obdulia, J. R. Bischoff, M. Albarran, A. Cebria, P. Alfonso, W. Link, J. Fominaya and J. Pastor, *Bioorg. Med. Chem. Lett.*, 2012, **22**, 1874–1878.
17 D. B. Belanger, M. J. Williams, P. J. Curran, A. K. Mandal, Z. Meng, M. P. Rainka, T. Yu, N. Y. Shih, M. A. Siddiqui, M. Liu, S. Tevar, S. Lee, L. Lianzhu, K. Gray, B. Yareko, J. Jones, E. B. Smith, D. B. Prelusky and A. D. Basso, *Bioorg. Med. Chem. Lett.*, 2010, **20**, 6739–6743.
18 S. A. Mitchell, M. D. Danca, P. A. Blomgren, J. W. Darrow, K. S. Currie, J. E. Kropf, S. H. Lee, S. L. Gallion, J. M. Xiong, D. A. Pippin, R. W. Desimone, D. R. Brittelli, D. C. Eustice, A. Bourret, M. Hill-Dezewi, P. M. Maciejewski and L. L. Elkin, *Bioorg. Med. Chem. Lett.*, 2009, **19**, 6991–6995.
19 X. Li and Y. Song, *Eur. J. Med. Chem.*, 2023, **260**, 115772.
20 (*a*) L. Yimin and W. Zhang, *QSAR Comb. Sci.*, 2004, **23**, 827–835; (*b*) A. Shaabani, E. Soleimani and J. Moghimi Rad, *Synth. Commun.*, 2008, **38**, 1090–1095; (*c*) M. I. Sarah, T. Heather and W. Mark, *Tetrahedron Lett.*, 2003, **44**, 4369–4371.
21 (*a*) S. K. Guchhait, C. Madaan and B. S. Thakkar, *Synthesis*, 2009, 3293–3300; (*b*) S. Guchhait and C. Madaan, *Synlett*, 2009, **4**, 628–632; (*c*) S. K. Guchhait and C. Madaan, *Tetrahedron Lett.*, 2011, **52**, 56–58.
22 (*a*) L. R. Amanda, M. Pulane and J. P. Christopher, *Tetrahedron Lett.*, 2007, **48**, 4079–4082; (*b*) M. Krasavin, S. Tsirulnikov, M. Nikulnikov, Y. Sandulenko and K. Bukhryakov, *Tetrahedron Lett.*, 2008, **49**, 7318–7321.
23 C. Blackburn, B. Guan, P. Fleming, K. Shiosaki and S. Tsai, *Tetrahedron Lett.*, 1998, **39**, 3635–3638.

24 L. R. Odell, M. Nilson, J. Gising, O. Lagerlund, D. Muthas, A. Nordqvist, A. Karlen and M. Larhed, *Bioorg. Med. Chem. Lett.*, 2009, **19**, 4790–4793.

25 (*a*) Y. M. Ren, C. Cai and R. C. Yang, *RSC Adv.*, 2013, **3**, 7182–7204; (*b*) A. T. Khan, M. M. Khan and K. K. R. Bannuru, *Tetrahedron*, 2010, **66**, 7762–7772; (*c*) A. T. Khan, A. Ghosh and M. M. Khan, *Tetrahedron Lett.*, 2012, **53**, 2622–2626.

26 (*a*) Z. T Bhutia, P. C. Panjikar, S. Iyer, A. Chatterjee and M. Banerjee, *ACS Omega*, 2020, **22**, 13333–13343; (*b*) U. Tekale Sunil, S. Kauthale Sushma, A. Dake Satish, R. Sarda Swapnil and P. Pawar Rajendra, *Curr. Org. Chem.*, 2012, **16**, 1385–2728; (*c*) L. Royer, S. K. De and R. A. Gibbs, *Tetrahedron Lett.*, 2005, **46**, 4595–4597; (*d*) J. Q. Wang, Z. Y. Zuo and W. He, *Catalysts*, 2022, **12**, 821; (*e*) S. S. Wu, C. T. Feng, D. Hu, Y. K. Huang, Z. Li, Z. G. Luo and S. T. Ma, *Org. Biomol. Chem.*, 2017, **15**, 1680–1685; (*f*) Y. Z. Yan, Y. Xu, B. Niu, H. F. Xie and Y. Q. Liu, *J. Org. Chem.*, 2015, **80**, 5581–5587.

27 (*a*) A. Parthiban, R. Sivasankar, B. Rajdev, R. N. Asha, T. C. Jeyakumar, R. Periakaruppan and V. G. M. Naidu, *J. Mol. Struct.*, 2022, **1270**, 133885; (*b*) A. Parthiban and P. Makam, *Bioorg. Chem.*, 2020, **105**, 104379; (*c*) P. Anaikutti, M. Selvaraj, J. Prabhakaran, T. Pooventhiran, T. C. Jeyakumar, R. Thomas and P. Makam, *J. Mol. Struct.*, 2022, **1266**, 133464; (*d*) A. Parthiban, J. Muthukumaran, A. Moushumi, S. Jayachandran, R. Krishna and H. S. P. Rao, *Med. Chem. Res*, 2014, **23**, 642–659; (*e*) A. Parthiban, M. Kumaravel, J. Muthukumaran, R. Rukkumani, R. Krishna and H. S. P. Rao, *Med. Chem. Res.*, 2015, **24**, 1226–1240; (*f*) A. Parthiban, M. Kumaravel, J. Muthukumaran, R. Rukkumani, R. Krishna and H. S. P. Rao, *Med. Chem. Res.*, 2016, **25**, 1308–1315; (*g*) A. Parthiban, J. Muthukumaran, A. Manhas, K. Srivastava, R. Krishna and H. S. P. Rao, *Bioorg. Med. Chem. Lett.*, 2015, **25**, 4657–4663.

28 G. S. Mani, S. P. Shaik, Y. Tangella, S. Bale, C. Godugu and A. Kamal, *Org. Biomol. Chem.*, 2017, **15**, 6780.

29 M. Umkehrer, G. Ross, N. Jager, C. Burdack, J. Kolb, H. Hu, M. Alvim Gaston and C. Hulme, *Tetrahedron Lett.*, 2007, **48**, 2213–2216.

30 G. Chauvière, B. Bouteille, B. Enanga de, C. Albuquerque, S. L. Croft, M. Dumas and J. Périé, *J. Med. Chem.*, 2003, **46**, 427–440.

31 P. Fernando da Silva Santos-Júnior, L. Rocha Silva, L. José Quintans-Júnior and E. Ferreira da Silva-Júnior, *Bioorg. Med. Chem. Lett.*, 2022, **75**, 128930.

32 (*a*) B. F. Lundt, N. L. Johansen, A. Vølund and J. Markussen, *Int. J. Pept. Protein Res.*, 1978, **12**, 258–268; (*b*) V. Evans, M. F. Mahon and R. L. Webster, *Tetrahedron*, 2014, **70**, 7593–7597; (*c*) J. D. Catt and W. L. Matier, *J. Org. Chem.*, 1974, **39**, 566–568; (*d*) P. Pollock, K. P. Cole, S. W. Roberts and M. Faul, *Org. Synth.*, 2012, **89**, 537–548.

33 (*a*) N. R. Chereddy, K. Suman, P. S. Korrapati, S. Thennarasu and A. B. Mandal, *Dyes Pigm.*, 2012, **95**, 606–613; (*b*) N. R. Chereddy, S. Thennarasu and A. B. Mandal, *Dalton Trans.*, 2012, **41**, 11753–11759.

34 (*a*) W. Jiasheng, L. Weimin, G. Jiechao, Z. Hongyan and W. Pengfei, *Chem. Soc. Rev.*, 2011, **40**, 3483–3495; (*b*) G. Aragay, J. Pons and A. Merkoc-I, *Chem. Rev.*, 2011, **111**, 3433.

35 G. H. Bae, S. Kim, N. K. Lee, A. Dagar, J. H. Lee, J. Lee and I. Kim, *RSC Adv.*, 2020, **10**, 7265–7288.

36 (*a*) R. Krishnamoorthy, M. Singh, A. Parthiban, P. L. Edwin, S. Dhanasekaran and T. Sathiah, *Bioorg. Chem.*, 2023, **134**, 106434; (*b*) S. Pajaniradje, M. K. Kumar, R. Radhakrishanan, S. A. Sufi, S. Subramaniam, P. Anaikutti, H. S. P. Rao and R. Rajagopalan, *Lett. Drug Des. Discovery*, 2020, **17**, 1146–1154.